BIOLOGY, MEDICINE, & NATURAL PRODUCT CHEMISTRY ISSN 2089-6514 (paper)
Volume 15, Number 1, April 2026 | Pages: 1575-1594 | DOI: 10.14421/biomedich.2026.151.1575-1594 ISSN 2540-9328 (online)

GC-MS Profiling and In Silico Antibacterial Activity of *Strobilanthes tonkinensis* Lindau Leaf Extracts via Maceration and Soxhlet Methods

Dwi Sapri Ramadhan[1]*, Dian Wardana[1], Hestia Hairima[2], Tita Juwitaningsih[1], Rosa Nadya Evelyn Sitorus[1], Vina Octavia Azzahra[3], Ilham Sinuraya[4]
[1]Department of Chemistry; [2]Department of Biology; [3]Department of Chemistry; [4]Biology Laboratory, Department of Biology; Faculty of Mathematics and Natural Sciences, Universitas Negeri Medan, Medan 20211, Indonesia.

Corresponding author*
dwisapri@unimed.ac.id

Manuscript received: 15 June 2026. Revision accepted: 07 July 2026, Published: 18 August 2026.

Abstract

Strobilanthes tonkinensis Lindau (Acanthaceae; locally known as daun paris) is an aromatic medicinal herb of Southeast Asian origin whose extraction-method-dependent secondary metabolite composition and antibacterial potential against defined molecular targets have not been systematically characterized. This study profiled the GC-MS-detectable metabolome of four leaf extracts obtained by ethanol maceration of fresh (3×24 h) and dried leaves (3×24 h), ethanol Soxhlet (13 cycles, 6.5 h), and n-hexane Soxhlet (25 cycles, 10 h) extraction of dried leaves, identifying 19, 27, 12, and 7 compounds, respectively. Extraction method and solvent polarity strongly governed compound class distribution: fresh ethanol maceration was dominated by 2-propionyl-1,4,5,6-tetrahydropyridine (33.21%) and cis-vaccenic acid (14.63%), while n-hexane Soxhlet selectively enriched stigmasterol to 67.95% of total peak area approximately 19-fold higher than ethanol maceration (3.61%). Five representative metabolites, stigmasterol, phytol, lupeol, squalene, and 2-propionyl-1,4,5,6-tetrahydropyridine were subjected to molecular docking against FtsA (PDB: 3WT0), OmpF (PDB: 4KR4), and DNA gyrase B (PDB: 6KZV), with ADMET profiling performed via SwissADME and ProTox 3.0. Lupeol (-8.0 kcal/mol) and stigmasterol (-7.7 kcal/mol) surpassed the native OmpF ligand binding affinity and demonstrated strong interaction with DNA gyrase B, supporting multi-target antibacterial potential. Squalene showed preferential affinity for FtsA (-7.1 kcal/mol). Among the candidates, 2-propionyl-1,4,5,6-tetrahydropyridine was the sole Lipinski-compliant compound with high predicted oral absorption, all five metabolites displayed no predicted hepatotoxicity or carcinogenicity. These findings identify lupeol and stigmasterol as priority antibacterial leads from *S. tonkinensis* and establish n-hexane Soxhlet extraction as an effective strategy for targeted phytosterol enrichment from this species.

Keywords: Acanthaceae; antibacterial; GC-MS; molecular docking; *Strobilanthes tonkinensis* Lindau.

Abbreviations: ADME, absorption distribution metabolism excretion; GC-MS, gas chromatography–mass spectrometry; PDB, Protein Data Bank; RT, retention time; AMR, antimicrobial resistance; GyrB, DNA gyrase subunit B; 2-THP, 2-propionyl-1,4,5,6-tetrahydropyridine; TPSA, topological polar surface area; MW, molecular weight

INTRODUCTION

The global crisis of antimicrobial resistance (AMR) poses an escalating public health threat, with an estimated 1.27 million deaths directly attributable to drug-resistant bacterial infections globally in 2019 (Murray et al., 2022). The emergence of multidrug-resistant pathogens including *Staphylococcus aureus*, *Escherichia coli*, and *Pseudomonas aeruginosa* has critically reduced the efficacy of conventional antibiotics, necessitating the urgent discovery of novel antimicrobial compounds (Puri et al., 2025; Salam et al., 2023; Steve et al., 2026). Medicinal plants continue to be a rich and underexplored reservoir of structurally diverse bioactive natural products that can serve as antimicrobial leads (Newman & Cragg, 2020).

The genus *Strobilanthes* (Acanthaceae) comprises over 450 species distributed across tropical and subtropical Asia, several of which have documented medicinal and pharmacological properties including antimicrobial, anti-inflammatory, antitumor, and antioxidant activities (Rawat et al., 2026). Among these, *Strobilanthes tonkinensis* Lindau locally known as "daun paris" is a fragrant perennial herb originating from Yunnan Province, China, and distributed throughout Southeast Asia including Thailand, Vietnam, and parts of Indonesia (Srikun, 2017; Suratman et al., 2022). The plant has been traditionally used as herbal tea and culinary spice owing to its characteristic glutinous rice-like aroma (Hua et al., 2022; X. Yang et al., 2025). Phytochemically, *S. tonkinensis* has been confirmed as a rich source of squalene (Wang et al., 2025), and reported

to possess antiviral, antitumor, anticoagulant, and anti-inflammatory activities (Zhu et al., 2022). The volatile metabolite profile of S. tonkinensis has recently been characterized, revealing 141 volatile metabolites dominated by alcohols, esters, and ketones (Hua et al., 2022). However, a systematic comparison of extraction methods on the lipophilic fraction and an in silico antibacterial evaluation against defined bacterial protein targets has not been reported.

GC–MS analysis is the principal tool for chemical profiling of volatile and semi-volatile plant metabolites, enabling identification of terpenes, fatty acids, and nitrogen-containing heterocycles relevant to antimicrobial research (Sarkar et al., 2024). Molecular docking combined with ADMET prediction provides a cost-effective strategy to prioritize bioactive compounds prior to experimental validation (Shamim et al., 2024; Warsito et al., 2021). Key bacterial targets evaluated in this study include FtsA (cell division protein), OmpF (outer membrane porin modulating antibiotic entry), and DNA gyrase B (topoisomerase essential for DNA replication) (Odoma et al., 2025; Sarkar et al., 2024).

Despite growing ethnopharmacological interest in *Strobilanthes tonkinensis*, no study has yet compared the effect of extraction method (maceration vs. Soxhlet, polar vs. non-polar solvent, fresh vs. dried leaf) on its secondary metabolite profile, nor performed an integrated in silico antibacterial evaluation of its GC-MS-identified compounds. The present study therefore aimed to: (1) characterize the GC-MS profile of four *S. tonkinensis* leaf extracts; (2) identify major bioactive candidates for in silico study; (3) evaluate their molecular interactions with FtsA, OmpF, and DNA gyrase via molecular docking; and (4) predict their pharmacokinetic and drug-likeness properties via ADMET analysis.

MATERIALS AND METHODS

Plant Material and Sample Preparation

Fresh leaves of *Strobilanthes tonkinensis* were collected from Semangat Gunung Village, Merdeka District, Karo Regency, North Sumatra, Indonesia (3°13'36.5"N 98°30'45.2"E) in March 2026. Voucher specimens were deposited at Herbarium Medanense USU under accession number 317/MEDA/2026. For fresh leaf maceration, leaves were washed, briefly air-dried at room temperature (28–32°C), and used directly. For dried leaf preparations, leaves were shade-dried at ambient temperature (28–32°C) for 48 h until constant weight was achieved, then ground to a homogeneous powder using a laboratory mill (particle size < 80 mesh). All solvents used (ethanol 96% and n-hexane) were of analytical grade (Merck, Germany).

Extraction

Maceration Method

Maceration was carried out in two treatments. Fresh leaf maceration: 200 g of fresh leaf material was immersed in 96% ethanol (1:10 w/v) in a sealed amber flask, macerated at room temperature with occasional stirring for 3×24 h. Dried leaf maceration: 100 g of powdered dried leaves was similarly macerated in 96% ethanol for 3×24 h. All macerates were filtered through Whatman No. 1 filter paper, pooled, and concentrated under reduced pressure at 40°C using a rotary evaporator (IKA RV10, Germany) to yield semi-solid extracts.

Soxhlet Method

Dried leaf powder (50 g per treatment) was subjected to Soxhlet extraction in 500 mL of solvent for 13 cycles over 6.5 h (ethanol) and 25 cycles for 10 h using a Soxhlet apparatus. Two solvent treatments were conducted sequentially: n-hexane extraction (to obtain non-polar fraction) followed by 96% ethanol extraction (to obtain semi-polar fraction). Both extracts were concentrated by rotary evaporation at 40°C and stored at 4°C prior to analysis.

GC-MS Analysis

Each extract was dissolved in n-hexane to a concentration of 10 mg/mL, filtered through a 0.45 µm PTFE syringe membrane filter, and analyzed using a Thermo Scientific™ ISQ™ 7610 single quadrupole GC-MS system (Thermo Fisher Scientific, Waltham, MA, USA) equipped with a TriPlus™ RSH autosampler and controlled by Thermo Scientific™ Chromeleon™ 7 Chromatography Data System (CDS) software (Version 7.3.2.10759).

Chromatographic separation was performed on a Thermo Scientific™ TG-1MS capillary column (30 m × 0.25 mm i.d. × 0.25 µm film thickness; non-polar, 100% polydimethylsiloxane stationary phase). Helium was used as carrier gas at a constant flow rate of 1.000 mL/min. Sample injection (1.0 µL) was performed in split mode with a split ratio of 50:1 (split flow 50.0 mL/min) and a purge flow of 5.000 mL/min. The injector temperature was set to 220°C. The oven temperature programme was as follows: initial temperature 40°C held for 4 min; first ramp at 8°C/min to 280°C; second ramp at 10°C/min to 300°C; final hold at 300°C for 14 min; total run time 50 min.

Mass spectrometric detection was performed in full scan Electron Ionization (EI) mode at 70 eV. The MS transfer line temperature was set to 250°C and the ion source temperature to 230°C. Spectra were acquired scan time of 0.2 s/scan (positive polarity, centroid spectrum type). Compound identification was carried out by matching acquired mass spectra against the NIST Mass Spectral Library (mainlib) integrated within the Chromeleon CDS, with a minimum acceptable similarity index (SI) of 700. Relative percentage composition of

each identified compound was calculated by peak area normalization without response factor correction.

Selection of Compounds for In Silico Study

Candidate compounds for molecular docking were selected based on four defined criteria applied cumulatively across all four extraction treatments: (1) relative peak area ≥ 1% in at least one extract, ensuring prioritization of compounds with meaningful abundance; (2) occurrence in a minimum of two independent extraction treatments, supporting plant-derived origin rather than extraction artifact or solvent contaminant; (3) confirmed identity as genuine plant secondary metabolites, explicitly excluding compounds attributable to solvent impurities (e.g., toluene, trimethylbenzene) or thermally induced rearrangement products under Soxhlet conditions; and (4) documented antibacterial activity through receptor-mediated or protein-binding mechanisms, as reported in the peer-reviewed literature, prioritizing compounds with molecular interactions relevant to the three selected target proteins. The three-dimensional structures of selected ligands were retrieved from the PubChem database in SDF format or drawn using Marvin Sketch 25.5.0 and optimized using the MMFF94 force field in OpenBabel 3.1.

Molecular Docking

Three bacterial target proteins were selected: (1) FtsA, a bacterial actin-like protein essential for cell division (PDB: 3WT0, *Staphylococcus aureus*) (Kato et al., 2015); (2) OmpF, the outer membrane porin of *Salmonella typhi* (PDB: 4KR4) (Madhuranayaki et al., 2014); and (3) DNA gyrase subunit B (GyrB) of *Escherichia coli* (PDB: 6KZV) (Mima & Ushiyama, 2020). These three targets were selected to represent distinct mechanisms of antibacterial action: FtsA as a target for disruption of bacterial cell division; OmpF as a determinant of outer membrane permeability relevant to Gram-negative pathogens, represented here by the *S. typhi* OmpF structure (4KR4) which shares high structural homology with E. coli OmpF; and DNA gyrase as a validated drug target for inhibition of DNA replication. Together, they enable evaluation of the selected compounds across complementary antibacterial pathways and both Gram-positive and Gram-negative bacterial contexts

Protein structures were downloaded from the RCSB Protein Data Bank (www.rcsb.org), processed in PyMOL: water molecules and heteroatoms were removed, polar hydrogen atoms and Gasteiger charges were added. Grid boxes were centered on co-crystallized ligand coordinates (FtsA: x=[4.991], y=[-6.306], z=[61.333], 16×20×23 Å; OmpF: x=[-28.250], y=[20.029], z=[-46.961], 15×19×16 Å; DNA gyrase: x=[-6.694], y=[15.125], z=[2.741], 19×13×18 Å). Molecular docking was performed using AutoDock Vina 1.2 (Trott & Olson, 2010). Binding energies (kcal/mol) and key protein–ligand interactions were analyzed using Discovery Studio Visualizer 2024. Co-crystallized reference ligands were re-docked as a validation step to confirm grid accuracy (RMSD ≤ 2.0 Å).

ADMET and Drug-likeness Prediction

The pharmacokinetic properties and drug-likeness of the selected compounds were predicted using SwissADME (http://www.swissadme.ch). Canonical SMILES retrieved from PubChem (https://pubchem.ncbi.nlm.nih.gov/) were used as input. Drug-likeness was evaluated based on Lipinski's Rule of Five, including molecular weight (MW), lipophilicity (XLogP3), hydrogen bond donors (HBD), hydrogen bond acceptors (HBA), and topological polar surface area (TPSA). Pharmacokinetic evaluation included gastrointestinal (GI) absorption and blood–brain barrier (BBB) permeability. Oral acute toxicity (LD50) was subsequently predicted using ProTox 3.0 (https://tox.charite.de/protox3/) (Banerjee et al., 2024). Compounds with more than one Lipinski violation were considered to have reduced oral drug-likeness.

RESULTS AND DISCUSSION

GC-MS Profile of Ethanol Maceration Extract from Fresh Leaves

GC–MS analysis was performed to characterize the chemical constituents present in the ethanol and n-hexane extracts of fresh and dried *Strobilanthes tonkinensis* leaves obtained by maceration and Soxhlet extraction. The resulting chromatographic profile enabled the identification of major and minor metabolites based on retention time, mass spectral data, and relative peak area percentages, providing an overview of the extract's chemical composition (Ramadhan et al., 2025).

GC-MS analysis of the ethanol maceration extract of fresh *S. tonkinensis* leaves (3×24 h) identified 19 compounds within a run time of 49.89 min, total ionic chromatogram (TIC) as shown in Figure 1, collectively representing 100% of total peak area (Table 1). The two most abundant compounds were 2-propionyl-1,4,5,6-tetrahydropyridine (33.21%; RT 15.395 min) and 2-propionyl-3,4,5,6-tetrahydropyridine (27.44%; RT 13.664 min). These two structural isomers together accounting for 60.65% of the total extract, are both tetrahydropyridine alkaloids and are the primary aroma-active compounds responsible for the characteristic glutinous rice-like fragrance of *S. tonkinensis*. Their predominance in the fresh leaf extract is consistent with the volatile metabolite profile reported by (Hua et al., (2022). Structurally, tetrahydropyridines (THP) derivatives have been reported to possess antimicrobial properties against various foodborne pathogens through disruption of bacterial metabolic processes (Chaudhary et al., 2026; Rossetti et al., 2019). THP derivatives have demonstrated activity against both Gram-positive and Gram-negative bacteria, as well as fungi. For instance, a

THP derivative (NUNL02) showed promising activity against *Mycobacterium abscessus*, significantly reducing the minimum inhibitory concentrations (MICs) of antibiotics like amikacin and ciprofloxacin when used in combination (Vianna et al., 2019).

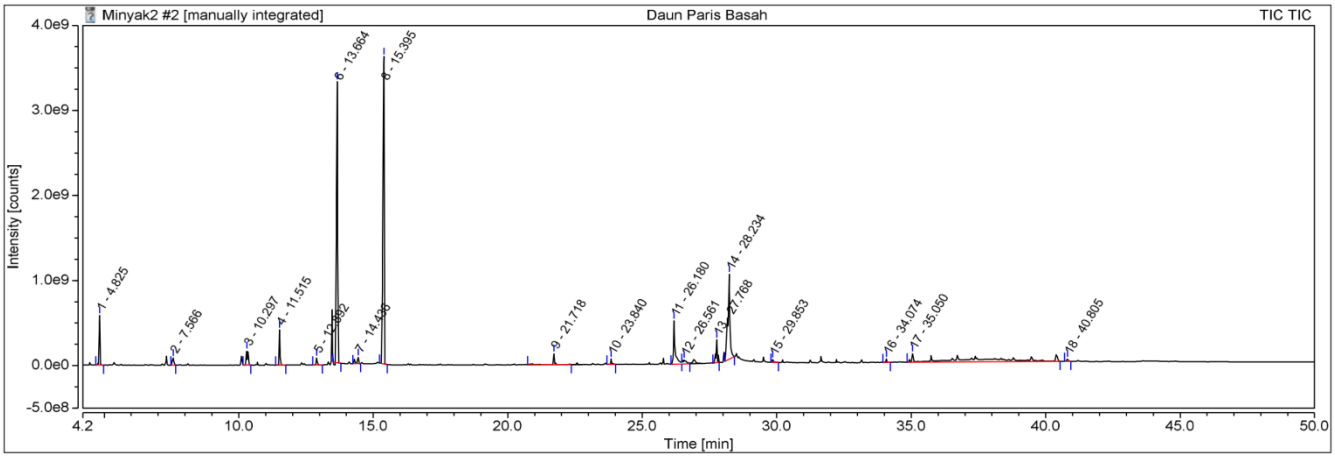

Figure 1. Total Ionic Chromatogram ethanol maceration extract of fresh *Strobilanthes tonkinensis.*

The third most abundant compound was cis-vaccenic acid (14.63%; RT 28.234 min), an omega-7 monounsaturated fatty acid (C18:1n-7). Vaccenic acid and its derivatives have demonstrated antibacterial activity against gram-positive bacteria by incorporating into bacterial membrane phospholipids, for instance, cis-vaccenic acid has been identified as a bioactive compound with antibacterial effects, potentially linked to its ability to disrupt bacterial cell structures or processes (Abdullah Sani et al., 2021; Karuppiah & Seralathan, 2022; Mohammad et al., 2025). n-Hexadecanoic acid (palmitic acid; 6.05%), a saturated C16 fatty acid ubiquitous in plant extracts, was also identified; its antimicrobial mechanism involves disruption of membrane integrity and inhibition of fatty acid biosynthesis (Desbois & Smith, 2010; Zulueta Díaz & Fanani, 2017). n-Hexadecanoic acid has been identified in various plant extracts and shown to exhibit moderate antimicrobial activity against bacteria such as *Staphylococcus aureus*, *Bacillus subtilis*, *Escherichia coli*, and *Klebsiella pneumoniae* (Ganesan et al., 2024). Additional compounds of bioactivity interest include 1-octen-3-ol (1.55%), a C8 alcohol fungicide and bacteriostat; phenylethyl alcohol (0.64%), a well-known broad-spectrum antimicrobial volatile; and lupeol (1.05%) and squalene (0.61%), terpenoids with documented antibacterial properties. The presence of toluene (3.33%) and xylene isomers (0.77%) is likely attributable to residual solvent volatiles rather than genuine secondary metabolites and should be interpreted with caution.

Table 1. GC-MS compounds identified in the ethanol maceration extract of fresh *Strobilanthes tonkinensis* leaves (3×24 h).

No.	RT (min)	Compound Name	Area (%)	MW (g/mol)	SI	Formula
1	3.995	Cyclohexane, methyl-	1.43	98	853	C_7H_{14}
2	4.825	Toluene	3.33	92	939	C_7H_8
3	7.566	o-Xylene	0.77	106	881	C_8H_{10}
4	10.297	1-Octen-3-ol	1.55	128	955	$C_8H_{16}O$
5	11.515	2-Acetyl-3,4,5,6-tetrahydropyridine	2.15	125	875	$C_7H_{11}NO$
6	12.892	Phenylethyl alcohol	0.64	122	901	$C_8H_{10}O$
7	13.664	2-Propionyl-3,4,5,6-tetrahydropyridine	27.44	139	887	$C_8H_{13}NO$
8	14.436	2-(2-Furyl)piperidine	0.69	151	679	$C_9H_{13}NO$
9	15.395	2-Propionyl-1,4,5,6-tetrahydropyridine*	33.21	139	884	$C_8H_{13}NO$
10	21.718	4-Dibutylaminobut-2-yn-1-ol	0.78	197	686	$C_{12}H_{23}NO$
11	26.180	n-Hexadecanoic acid (Palmitic acid)	6.05	256	919	$C_{16}H_{32}O_2$
12	26.561	Dasycarpidan-1-methanol, acetate (ester)	1.14	326	719	$C_{20}H_{26}N_2O_2$
13	26.928	Tertbutyloxyformamide, N-methyl-N-[4-(1-pyrrolidinyl)-2-butynyl]-	1.11	252	677	$C_{14}H_{24}N_2O_2$
14	27.768	9,12,15-Octadecatrienoic acid, methyl ester (Z,Z,Z)	2.17	292	924	$C_{19}H_{32}O_2$
15	28.234	cis-Vaccenic acid	14.63	282	905	$C_{18}H_{34}O_2$
16	31.646	9-Octadecenoic acid (Z)-, oxiranylmethyl ester	0.65	338	889	$C_{21}H_{38}O_3$
17	35.050	Squalene*	0.61	410	778	$C_{30}H_{50}$

No.	RT (min)	Compound Name	Area (%)	MW (g/mol)	SI	Formula
18	37.380	Octadecane, 3-ethyl-5-(2-ethylbutyl)-	0.60	366	685	$C_{26}H_{54}$
19	40.393	Lupeol*	1.05	426	789	$C_{30}H_{50}O$

Asterisk (*) indicates compounds selected for molecular docking. RT=retention time, MW=molecular weight, SI=similarity index.

GC-MS Profile of Ethanol Maceration Extract from Dried Leaves

GC–MS analysis of the ethanol maceration extract of dried *Strobilanthes tonkinensis* leaves resulted in the identification of twenty-seven compounds. The TIC is presented in Figure 2, and the corresponding compounds are summarized in Table 2. The compound profile shifted substantially compared to the fresh leaf extract, reflecting both the concentration of non-volatile constituents upon drying and partial ester hydrolysis during the drying process. The dominant compound was 9-octadecenoic acid (Z)-, oxiranylmethyl ester (glycidyl oleate; 14.15%; RT 31.295 min), a fatty acid epoxide derivative with documented cytotoxic and antimicrobial properties (Fatmayanti et al., 2024; J. Kim et al., 2024). Phytol (11.31%; RT 28.034 min), a diterpene alcohol and chlorophyll degradation product, emerged as the second most abundant compound. Phytol has been extensively reported for its antimicrobial activity against both gram-positive and gram-negative bacteria, acting through membrane disruption and inhibition of lipid biosynthesis (Almeida-Bezerra et al., 2024; Lee et al., 2016; Murugan et al., 2025). Its higher abundance in the dried extract relative to fresh leaves reflects the release of phytol from chlorophyll during the drying process.

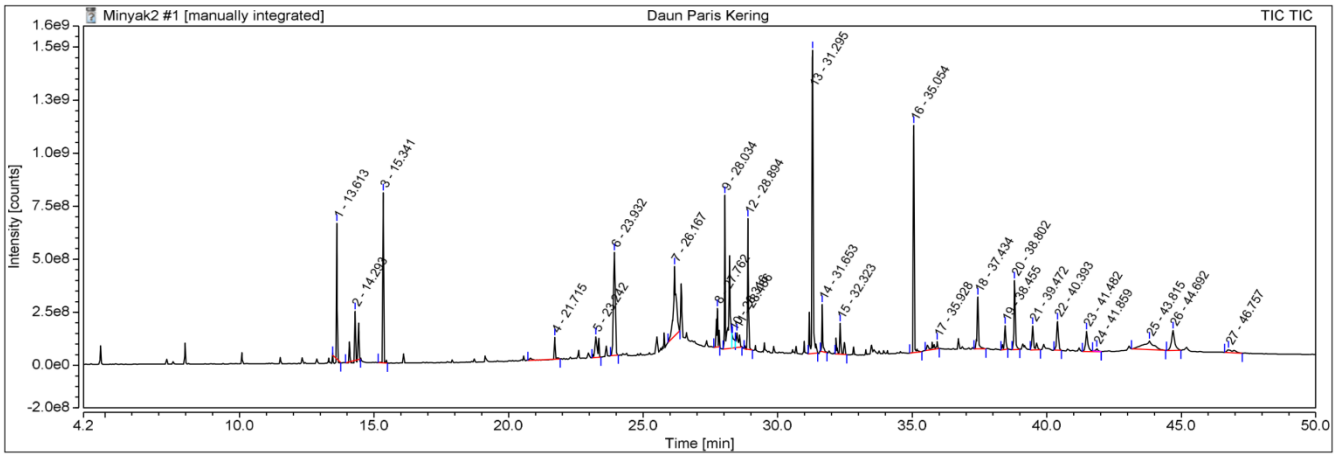

Figure 2. Total Ionic Chromatogram ethanol maceration extract of dried *Strobilanthes tonkinensis.*

Squalene (7.35%; RT 35.054 min) was considerably more abundant in the dried leaf extract than in the fresh (0.61%), an increase attributable to the preferential removal of highly volatile constituents (notably water and tetrahydropyridine alkaloids) during the drying process, which proportionally elevates the relative representation of non-volatile lipophilic compounds in the dried extract rather than an absolute increase in squalene content. Squalene is the signature compound of *S. tonkinensis* (Wang et al., 2025) and functions as an antimicrobial agent by interfering with the bacterial cell membrane and sterol biosynthesis pathway (Raghavanpillai Sabu et al., 2022; R. Yang et al., 2018). n-Hexadecanoic acid (palmitic acid; 7.78%), 9-octadecenoic acid methyl ester (oleic acid methyl ester; 7.79%), stigmasterol (3.61%), dl-α-tocopherol (2.71%), campesterol (1.47%), and lupeol (2.25%) were also identified. The phytosterols stigmasterol and campesterol, together with the pentacyclic triterpenoid lupeol, constitute a lipophilic bioactive fraction consistent with reported profiles in other *Strobilanthes* species (Rawat et al., 2026). The propionyl-tetrahydropyridine isomers were detected at considerably lower percentages (2.93% and 5.10% combined) compared to the fresh leaf extract, supporting their predominantly volatile nature and susceptibility to loss during the drying process. Multiple peaks attributable to 9-octadecenoic acid (Z)-, oxiranylmethyl ester at various retention times (peaks 23–27; 9.71% cumulative) suggest thermal rearrangement of glycidyl esters or co-elution artifacts that warrant consideration in compound quantification.

Table 2. GC-MS compounds identified in the ethanol maceration extract of dried *Strobilanthes tonkinensis* leaves (3×24 h).

No.	RT (min)	Compound Name	Area (%)	MW (g/mol)	SI	Formula
1	13.613	2-Propionyl-3,4,5,6-tetrahydropyridine	2.93	139	896	$C_8H_{13}NO$
2	14.293	Butan-2-one, 4-[pyrrolidin-2-one-5-yl]-	2.72	155	757	$C_8H_{13}NO_2$
3	15.341	2-Propionyl-1,4,5,6-tetrahydropyridine*	5.10	139	894	$C_8H_{13}NO$
4	21.715	2-Ethylcyclohexylamine, N-(2-chloropropylidene)-, N-oxide	0.93	217	678	$C_{11}H_{20}ClNO$
5	23.242	9,12-Octadecadienoic acid (Z,Z)-, methyl ester	2.47	294	881	$C_{19}H_{34}O_2$
6	23.932	9-Octadecenoic acid (Z)-, methyl ester	7.79	296	940	$C_{19}H_{36}O_2$
7	26.167	n-Hexadecanoic acid (Palmitic acid)	7.78	256	783	$C_{16}H_{32}O_2$
8	27.762	9,12,15-Octadecatrienoic acid, methyl ester (Z,Z,Z)	2.37	292	857	$C_{19}H_{32}O_2$
9	28.034	Phytol*	11.31	296	917	$C_{20}H_{40}O$
10	28.316	cis-13-Octadecenoic acid	1.31	282	854	$C_{18}H_{34}O_2$
11	28.486	trans-13-Octadecenoic acid	1.47	282	815	$C_{18}H_{34}O_2$
12	28.894	Glycidyl palmitate	5.13	312	933	$C_{19}H_{36}O_3$
13	31.295	9-Octadecenoic acid (Z)-, oxiranylmethyl ester	14.15	338	896	$C_{21}H_{38}O_3$
14	31.653	Glycidol stearate	1.91	340	841	$C_{21}H_{40}O_3$
15	32.323	Thiocarbamic acid, N,N-dimethyl, S-1,3-diphenyl-2-butenyl ester	2.34	311	765	$C_{19}H_{21}NOS$
16	35.054	Squalene*	7.35	410	933	$C_{30}H_{50}$
17	35.928	1-Heptatriacotanol	1.15	536	758	$C_{37}H_{76}O$
18	37.434	dl-α-Tocopherol	2.71	430	700	$C_{29}H_{50}O_2$
19	38.455	Campesterol	1.47	400	751	$C_{28}H_{48}O$
20	38.802	Stigmasterol*	3.61	412	839	$C_{29}H_{48}O$
21	39.472	Cholest-22-ene-21-ol, 3,5-dehydro-6-methoxy-, pivalate	1.80	498	735	$C_{33}H_{54}O_3$
22	40.393	Lupeol*	2.25	426	817	$C_{30}H_{50}O$
23	41.482–46.757	9-Octadecenoic acid (Z)-, oxiranylmethyl ester (multiple)	9.71	338	694-743	$C_{21}H_{38}O_3$

Asterisk (*) indicates compounds selected for molecular docking. RT=retention time, MW=molecular weight, SI=similarity index.

GC-MS Profile of Ethanol Soxhlet Extract from Dried Leaves

GC–MS analysis of the ethanol Soxhlet extract obtained from dried *S. tonkinensis* leaves (13 extraction cycles, 6.5 h) resulted in the identification of 12 compounds. The total ion chromatogram is presented in Figure 3, while the identified compounds are listed in Table 3. Among these, 2-piperidinecarboxamide (pipecolic acid amide) was the predominant constituent, accounting for 59.79% of the total peak area at a retention time of 14.290 min. This nitrogen-containing heterocycle has not been previously reported as a major compound in *S. tonkinensis* and may represent either a genuine secondary metabolite of the species or a thermally induced rearrangement product generated under the elevated temperatures of Soxhlet extraction (Yuan et al., 2017). 2-Piperidinecarboxamide is structurally related to pipecolic acid, a non-protein amino acid with established antimicrobial and immunomodulatory properties (Al-Rooqi et al., 2022; Hartmann et al., 2017). The thermal conditions of Soxhlet extraction (reflux temperature of ethanol ~78°C) may have promoted Maillard-type condensation reactions between amino acids and reducing sugars in the dried leaf matrix, generating piperidine-ring compounds that are not native to the fresh plant.

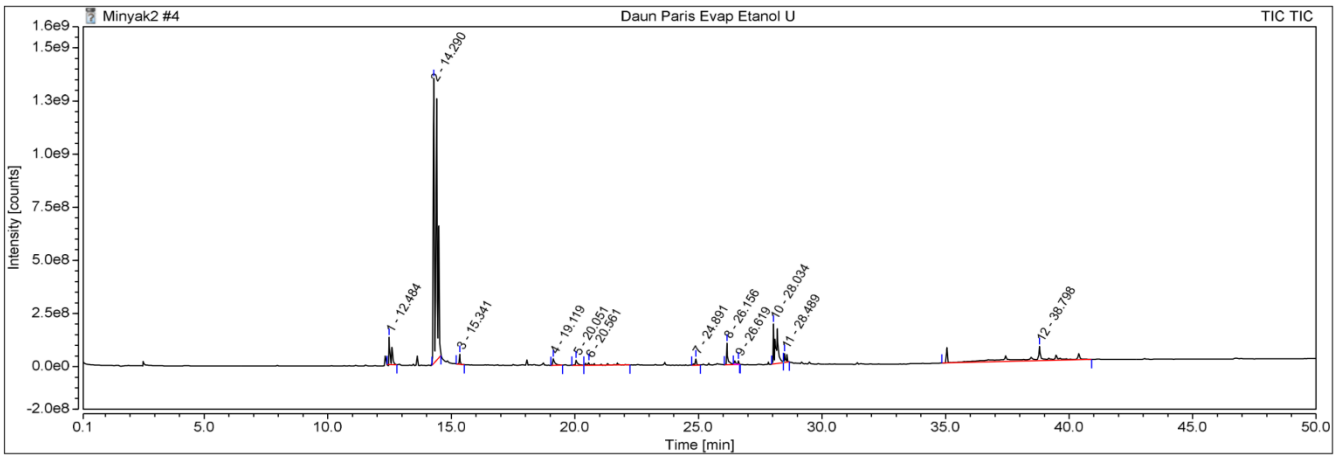

Figure 3. Total Ionic Chromatogram of the ethanol Soxhlet extract of dried *Strobilanthes tonkinensis* leaves (6.5 h).

Stigmasterol was the second most abundant compound (18.09%), markedly higher than in the dried maceration extract (3.61%), reflecting the enhanced extraction efficiency of Soxhlet for high-molecular-weight, thermostable phytosterols. Phytol (9.69%) was also well-represented. The reduced compound diversity (12 vs. 27 compounds) compared to maceration may reflect the selective extraction under continuous thermal conditions, favoring thermally stable lipophilic compounds while volatilizing labile low-MW constituents. n-Hexadecanoic acid (2.37%) and 2-propionyl-1,4,5,6-tetrahydropyridine (0.64%) were detected at reduced abundances relative to maceration extracts.

Table 3. GC-MS compounds identified in the ethanol Soxhlet extract of dried *Strobilanthes tonkinensis* leaves (13 cycles, 6.5 h).

No.	RT (min)	Compound Name	Area (%)	MW (g/mol)	SI	Formula
1	12.484	1-(Piperidin-2-yl)ethan-1-ol	3.61	129	909	$C_7H_{15}NO$
2	14.290	2-Piperidinecarboxamide	59.79	128	928	$C_6H_{12}N_2O$
3	15.341	2-Propionyl-1,4,5,6-tetrahydropyridine*	0.64	139	810	$C_8H_{13}NO$
4	19.119	Phenol, 2,3,5,6-tetramethyl-	1.13	150	791	$C_{10}H_{14}O$
5	20.051	Pyrazolo[1,5-a]pyridine, 3,3a,4,7-tetrahydro-2,3,3-trimethyl-	0.93	164	738	$C_{10}H_{16}N_2$
6	20.561	6-Nonyl-5,6-dihydro-2H-pyran-2-one	1.21	224	679	$C_{14}H_{24}O_2$
7	24.891	Ethanol, 2-(9-octadecenyloxy)-, (Z)-	0.68	312	817	$C_{20}H_{40}O_2$
8	26.156	n-Hexadecanoic acid (Palmitic acid)	2.37	256	904	$C_{16}H_{32}O_2$
9	26.619	Hexadecanoic acid, ethyl ester	0.52	284	785	$C_{18}H_{36}O_2$
10	28.034	Phytol*	9.69	296	918	$C_{20}H_{40}O$
11	28.489	Butyl 9,12-octadecadienoate	1.35	336	816	$C_{22}H_{40}O_2$
12	38.798	Stigmasterol*	18.09	412	753	$C_{29}H_{48}O$

Asterisk (*) indicates compounds selected for molecular docking. RT=retention time, MW=molecular weight, SI=similarity index.

GC-MS Profile of n-Hexane Soxhlet Extract from Dried Leaves

The n-hexane Soxhlet extract (25 extraction cycles, 10 h) yielded the least complex profile, with only 7 compounds identified (Table 4). Stigmasterol was overwhelmingly dominant (67.95%; RT 38.805 min), constituting nearly 68% of the total peak area. This exceptionally high abundance confirms the high lipophilicity of stigmasterol and underscores the selectivity of n-hexane for non-polar phytosterols. Phytol was the second major compound (13.23%). The highly simplified profile in comparison to ethanol extracts is consistent with the narrow polarity range of n-hexane, which selectively dissolves waxes, terpenes, and sterols while excluding polar metabolites (Abedelmaksoud et al., 2025; Azzahra et al., 2025).

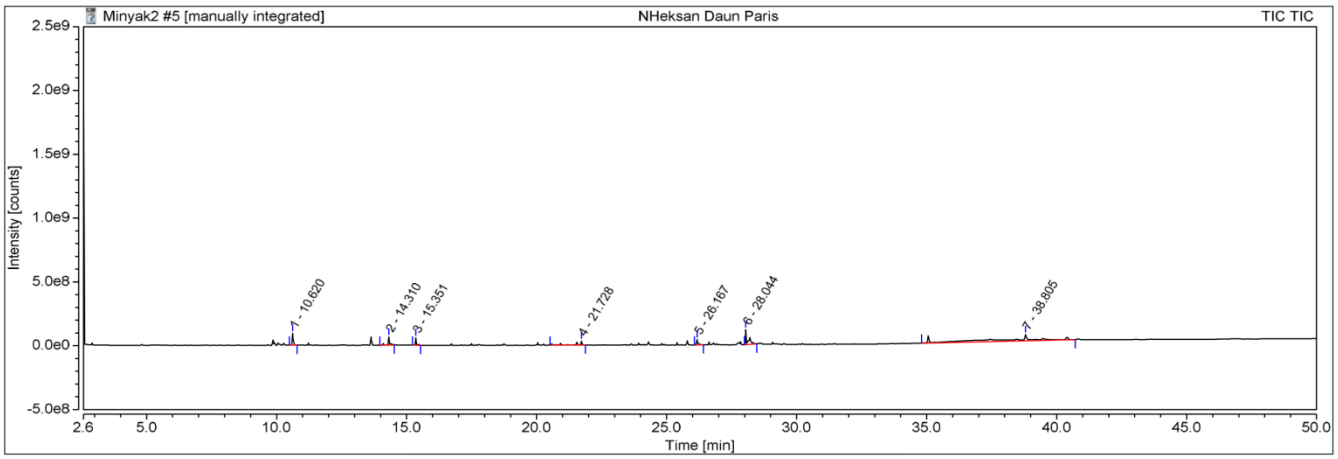

Figure 4. Total Ionic Chromatogram of the n-hexane Soxhlet extract of dried *Strobilanthes tonkinensis* leaves (10 h).

Notably, 2-propionyl-1,4,5,6-tetrahydropyridine (2.75%) was detected even in the n-hexane extract, suggesting partial lipophilic character of this compound. The presence of benzene-1,2,4-trimethyl (3.77%) likely reflects solvent impurities rather than genuine phytochemical content. The striking dominance of stigmasterol in the n-hexane fraction validates the use of this solvent specifically for phytosterol enrichment in *S. tonkinensis*. Stigmasterol is a C29 phytosterol with a broad spectrum of biological activities including antibacterial, anti-inflammatory, and anticancer properties, operating through multiple mechanisms such

as membrane disruption and inhibition of bacterial sterol biosynthesis (Bakrim et al., 2022; Lestari et al., 2024; Morgan et al., 2021). Stigmasterol is a C29 phytosterol with documented antibacterial activity mediated through inhibition of MurA, PBP, and membrane disruption (Bakrim et al., 2022). Additionally, stigmasterol derivatives have shown antibacterial effects in food preservation systems (U. Khan et al., 2023; Y. A. Kim & Kim, 2025).

Table 4. GC-MS compounds identified in the n-hexane Soxhlet extract of dried *Strobilanthes tonkinensis* leaves (25 cycles, 10 h).

No.	RT (min)	Compound Name	Area (%)	MW (g/mol)	SI	Formula
1	10.620	Benzene, 1,2,4-trimethyl-	3.77	120	928	C_9H_{12}
2	14.310	1-(Piperidin-2-yl)propan-1-one	4.35	141	929	$C_8H_{15}NO$
3	15.351	2-Propionyl-1,4,5,6-tetrahydropyridine*	2.75	139	862	$C_8H_{13}NO$
4	21.728	2-Ethylcyclohexylamine, N-(2-chloropropylidene)-, N-oxide	4.76	217	689	$C_{11}H_{20}ClNO$
5	26.167	n-Hexadecanoic acid (Palmitic acid)	3.18	256	870	$C_{16}H_{32}O_2$
6	28.044	Phytol*	13.23	296	907	$C_{20}H_{40}O$
7	38.805	Stigmasterol*	67.95	412	681	$C_{29}H_{48}O$

Asterisk (*) indicates compounds selected for molecular docking. RT=retention time, MW=molecular weight, SI=similarity index.

Comparative Analysis of Extraction Methods and Compound Selection for In Silico Study

Comparative analysis of the four extraction protocols was conducted to evaluate the influence of extraction method and solvent polarity on the metabolite composition of *S. tonkinensis* leaves. Variations in the number, abundance, and chemical classes of detected compounds were assessed to identify the most representative bioactive metabolites. Based on their relative abundance, structural diversity, reported biological activities, and suitability for molecular docking, selected major compounds were subsequently chosen for in silico antibacterial evaluation against FtsA, OmpF, and DNA gyrase target proteins.

First, drying the leaves prior to extraction significantly expanded the compound profile (from 19 to 27 compounds in maceration) and shifted the dominant class from volatile nitrogen-containing heterocycles (tetrahydropyridines) to fatty acid esters, phytosterols, and terpenoids. This reflects both the concentration of lipophilic secondary metabolites and the enzymatic/thermal conversion of chlorophylls to phytol. Second, n-hexane soxhlet extraction produced the highest stigmasterol content (67.95%), which was approximately 19 times higher than that obtained by ethanol maceration of dried leaves (3.61%) and nearly four times higher than that obtained by ethanol Soxhlet extraction (18.09%). This observation highlights the critical role of solvent polarity and extraction conditions in enhancing phytosterol extraction efficiency. Third, squalene a biosynthetic marker of *S. tonkinensis* was exclusively detected in maceration extracts (0.61% fresh, 7.35% dried), suggesting its loss or decomposition under the high-temperature conditions of Soxhlet extraction.

Based on these analyses, five compounds satisfying all applicable criteria were ultimately selected for in silico evaluation (Table 5): stigmasterol, phytol, lupeol, squalene, and 2-propionyl-1,4,5,6-tetrahydropyridine. This set spans five distinct chemical classes a C29 phytosterol, a diterpene alcohol, a pentacyclic triterpenoid, a triterpene hydrocarbon, and a nitrogen-containing bicyclic heterocycle providing structural diversity for probing different binding mechanisms against the three bacterial target proteins selected. The chemical structures of these selected compounds are presented in Figure 5.

Table 5. Compounds selected from GC-MS analysis of *Strobilanthes tonkinensis* extracts for molecular docking against FtsA (3WT0), OmpF (4KR4), and DNA gyrase (6KZV).

No.	Compound	Formula	MW	Presence in Extract	Reported Activity
1	Stigmasterol	$C_{29}H_{48}O$	412.69	All extracts; dominant in n-hexane Soxhlet (67.95%)	Antibacterial via MurA and PBP inhibition; membrane disruption; antifungal (Kurnia et al., 2020; Lestari et al., 2024)
2	Phytol	$C_{20}H_{40}O$	296.53	Dried leaf extracts; highest in n-hexane Soxhlet (13.23%)	Antibacterial against MDR *Klebsiella pneumoniae* via membrane disruption and DNA gyrase inhibition; antibiotic potentiator (Almeida-Bezerra et al., 2024; Murugan et al., 2025)
3	Lupeol	$C_{30}H_{50}O$	426.72	Both maceration extracts (1.05–2.25%)	Antibacterial against *S. aureus* and *E. coli*; anti-inflammatory; cell wall synthesis inhibitor (T. Khan et al., 2025; Park et al., 2024)
4	Squalene	$C_{30}H_{50}$	410.72	Fresh and dried maceration	Antibacterial via membrane integrity

No.	Compound	Formula	MW	Presence in Extract	Reported Activity
				(0.61–7.35%)	disruption; characteristic marker compound of *S. tonkinensis* (Sri Charan Bindu et al., 2015; Wang et al., 2025)
5	2-Propionyl-1,4,5,6-tetrahydropyridine	$C_8H_{13}NO$	139.20	All four extracts; dominant in fresh maceration (33.21%)	Antimicrobial heterocyclic scaffold, characteristic aroma (Susawaengsup et al., 2022)

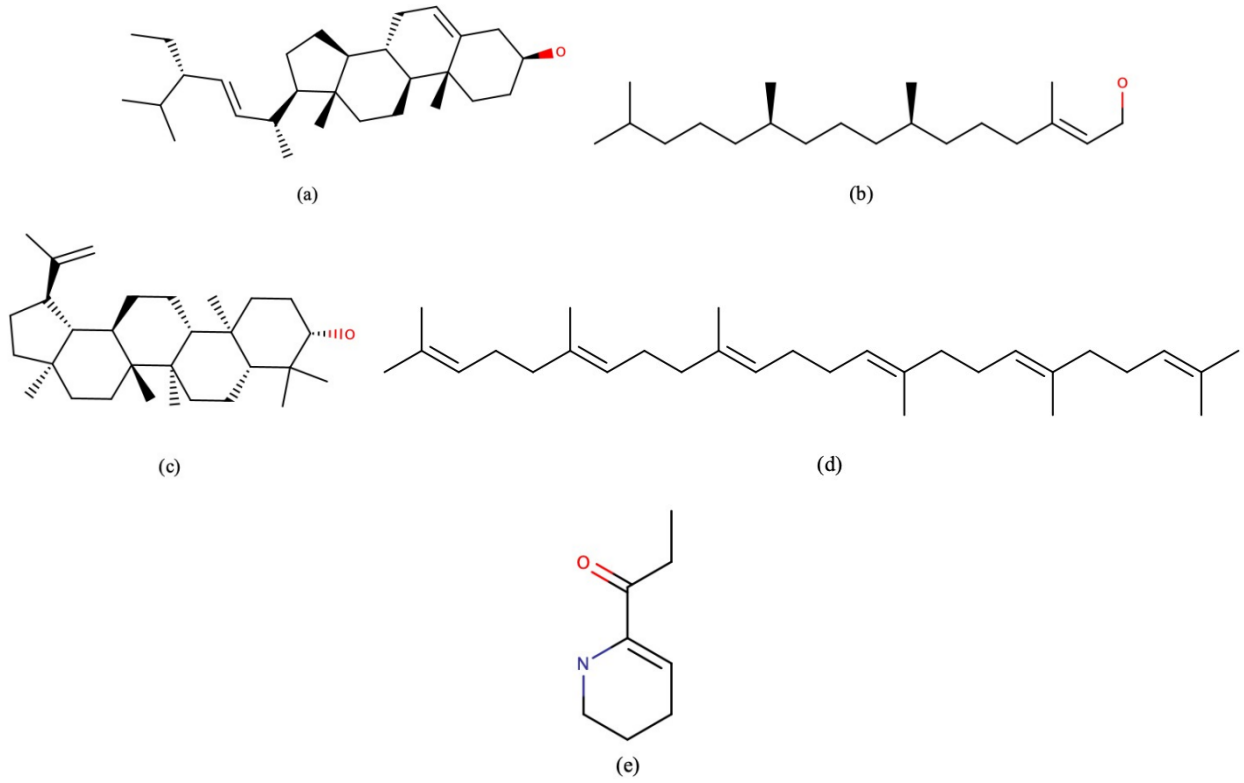

Figure 5. Chemical structures of (a) stigmasterol, (b) phytol, (c) lupeol, (d) squalene, and (e) 2-propionyl-1,4,5,6-tetrahydropyridine selected for in silico antibacterial evaluation.

Applying selection four defined criteria, several highly abundant compounds were intentionally excluded. 2-Piperidinecarboxamide (59.79% in ethanol Soxhlet extract) was excluded on the basis of criteria 2 and 3: it appeared exclusively in the ethanol Soxhlet fraction and likely represents a thermally induced Maillard-type rearrangement product of pipecolic acid or related amino acids generated under the reflux conditions of Soxhlet extraction (Yuan et al., 2017), rather than an inherent secondary metabolite of *S. tonkinensis*. 9-Octadecenoic acid (Z)-, oxiranylmethyl ester (glycidyl oleate; 14.15% primary peak in dried maceration) was excluded based on criteria 2 and 3: its appearance at five distinct retention times (RT 31.295, 31.653, 41.482, 43.815, and 44.692 min) in the dried maceration extract strongly indicates thermal decomposition or co-elution artifacts rather than a stable, discretely identifiable compound suitable for molecular docking. n-Hexadecanoic acid (palmitic acid), although present across all four extracts (2.37–7.78%), was excluded based on criterion 4: its primary antibacterial mechanism operates through non-specific membrane disruption rather than defined protein–receptor interactions (Desbois & Smith, 2010), rendering it unsuitable for structure-based docking against the protein targets examined. Similarly, cis-vaccenic acid was excluded on the same mechanistic basis. Of the two propionyl-tetrahydropyridine structural isomers detected (2-propionyl-3,4,5,6-tetrahydropyridine and 2-propionyl-1,4,5,6-tetrahydropyridine), only 2-propionyl-1,4,5,6-tetrahydropyridine was selected as the representative candidate, given its higher cumulative abundance across all four extracts (present at 33.21%, 5.10%, 0.64%, and 2.75%) and its status as the most abundant single compound in the fresh maceration extract; the closely related isomer shares an identical molecular formula and mass spectrum, making independent docking evaluation redundant.

Molecular Docking Analysis

Molecular docking was performed to evaluate the potential binding interactions of five GC-MS-identified compounds from *Strobilanthes tonkinensis* against three bacterial target proteins implicated in distinct antibacterial mechanisms: FtsA (PDB: 3WT0), OmpF

(PDB: 4KR4), and DNA gyrase subunit B, GyrB (PDB: 6KZV). In molecular docking, a more negative binding free energy (ΔG, expressed in kcal/mol) indicates stronger non-covalent interactions between the ligand and the receptor binding site, reflecting greater thermodynamic favorability of complex formation (Liu et al., 2022). Based on widely applied thresholds in the natural product docking literature, binding affinities ranging from -5.0 to -7.0 kcal/mol are generally classified as moderate, those from -7.0 to -9.0 kcal/mol as good to strong, and values below -9.0 kcal/mol as very strong (Boufissiou et al., 2025; Hartavi, 2025; Yasir et al., 2025). The binding affinity scores of all five compounds against the three receptors, together with their respective native co-crystallized ligands as reference controls, are summarized in Figure 6.

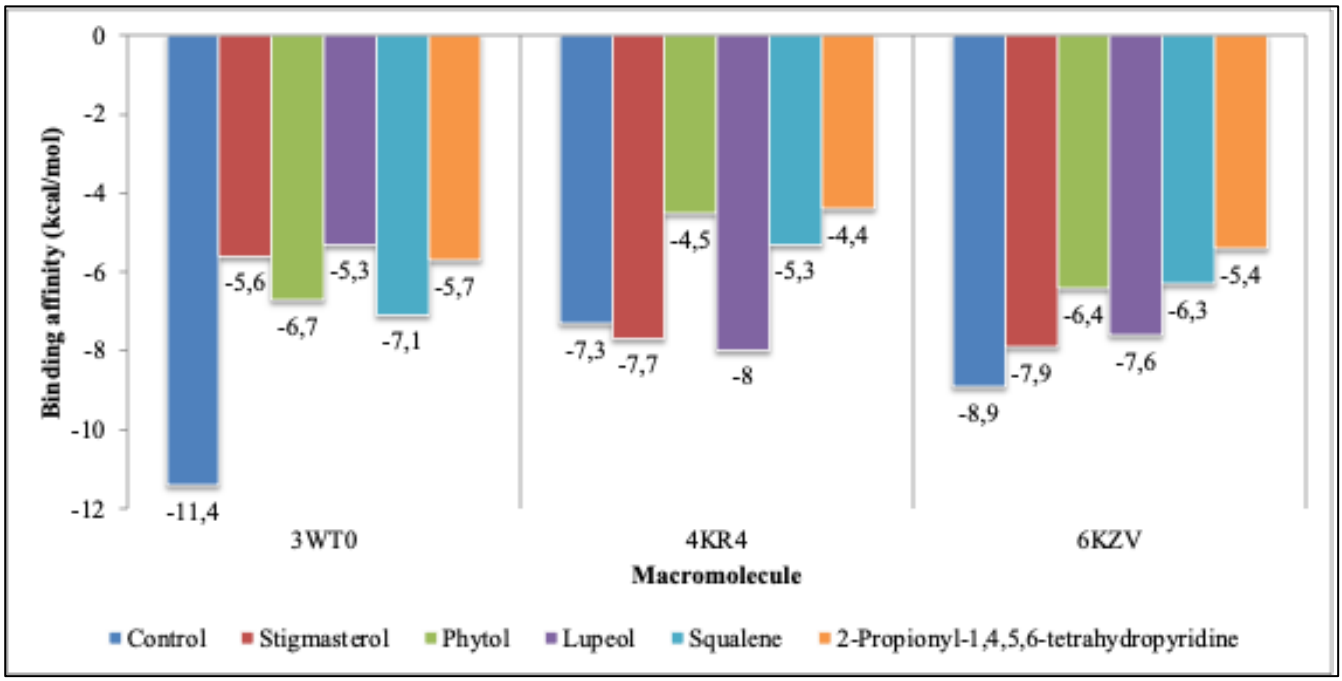

Figure 6. Binding affinity values of the selected compounds and native co-crystallized ligands against FtsA (3WT0), OmpF (4KR4), and DNA gyrase subunit B (6KZV) obtained from molecular docking analysis.

The overall data reveal a compound and target-dependent pattern of binding affinities. Against FtsA (3WT0), squalene demonstrated the strongest interaction among the test compounds (-7.1 kcal/mol), followed by phytol (-6.7 kcal/mol), 2-propionyl-1,4,5,6-tetrahydropyridine (2-THP; -5.7 kcal/mol), stigmasterol (-5.6 kcal/mol), and lupeol (-5.3 kcal/mol), all of which remained weaker than the native ligand (-11.4 kcal/mol). Against OmpF (4KR4), a particularly notable finding was that both lupeol (-8.0 kcal/mol) and stigmasterol (-7.7 kcal/mol) surpassed the binding affinity of the native ligand (-7.3 kcal/mol), indicating competitive or superior occupancy of the receptor binding site. Against GyrB (6KZV), stigmasterol exhibited the strongest affinity (-7.9 kcal/mol), closely followed by lupeol (-7.6 kcal/mol), with phytol (-6.4 kcal/mol), squalene (-6.3 kcal/mol), and 2-THP (-5.4 kcal/mol) demonstrating progressively weaker but nonetheless pharmacologically relevant interactions. Taken collectively, these data suggest that lupeol and stigmasterol possess the broadest multi-target binding potential, while squalene shows preferential affinity for FtsA, and 2-THP exhibits generally weaker interactions across all three targets.

Binding at FtsA (PDB: 3WT0)

FtsA is a bacterial actin-like ATPase that functions as an essential organizer of the divisome complex, anchoring the tubulin homologue FtsZ to the cytoplasmic membrane and coordinating Z-ring constriction during cytokinesis (Cameron & Margolin, 2023). The amino acid residues involved in the interactions between the selected compounds and FtsA (3WT0) are summarized in Table 6. These interactions include hydrogen bonds, van der Waals forces, alkyl interactions, and electrostatic contacts that contribute to ligand binding within the active site. The native ligand of 3WT0 forms an extensive network of ten conventional hydrogen bonds with the ATP-binding domain residues SER13, SER14, SER15, GLU209, VAL211, ASP210, GLY325, LYS254, GLU251, and ASN328, in addition to carbon hydrogen bonds at SER326 and GLY208, and critical electrostatic interactions at LYS17 and the catalytic magnesium ion MG401 via salt bridges. This rich interaction profile accounts for the very strong native ligand affinity of -11.4 kcal/mol.

Table 6. Detailed ligand–protein interaction analysis of the selected compounds and native ligand within the binding pocket of 3WT0.

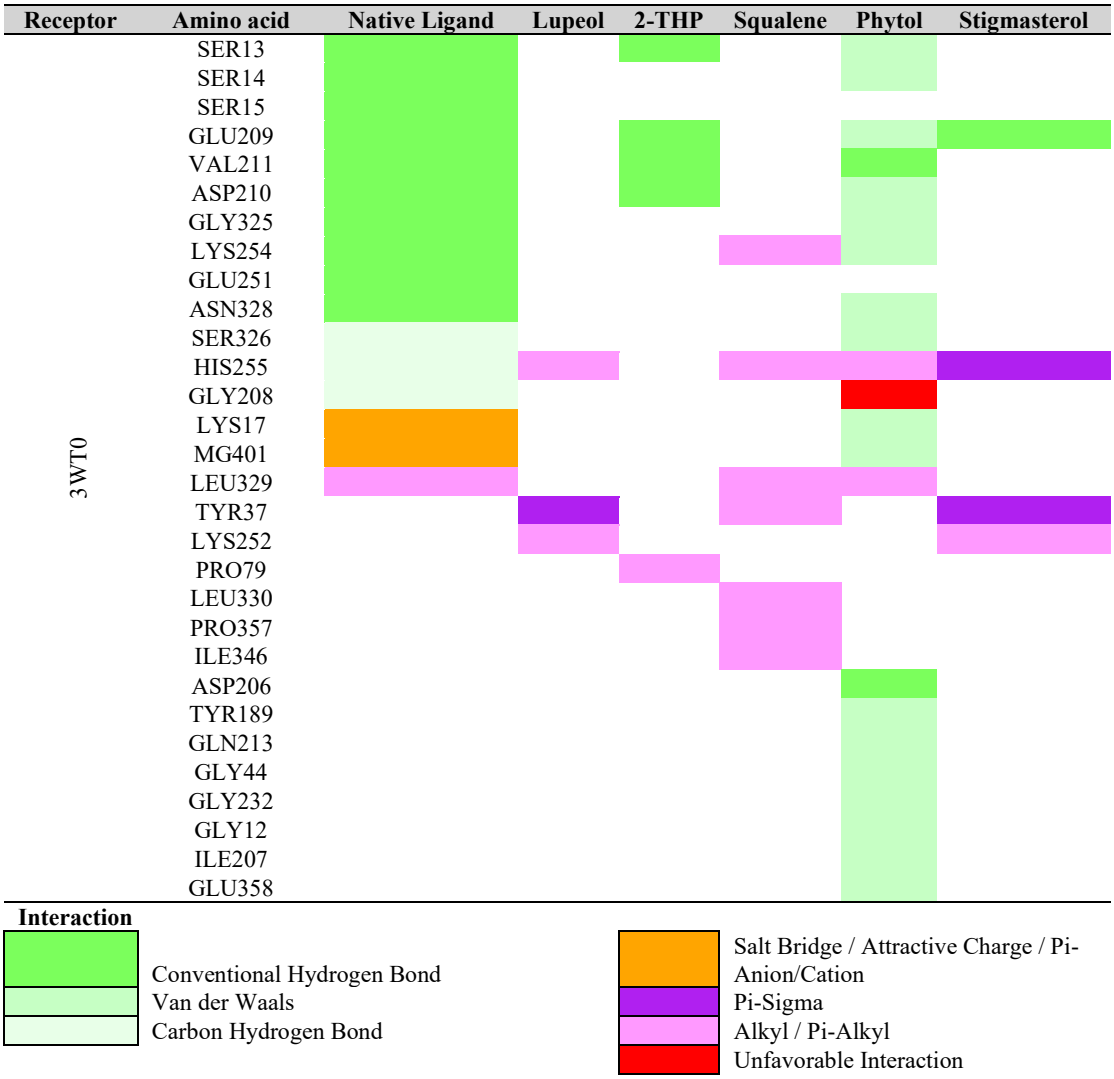

Among the test compounds, squalene achieved the strongest binding at FtsA (-7.1 kcal/mol) through a predominantly hydrophobic mechanism as illustrated in Figure 7. It engaged LYS254 and HIS255 via alkyl and pi-alkyl interactions, while extending contacts to LEU329, LEU330, PRO357, ILE346, and TYR37, forming a broad hydrophobic interface throughout the ligand-binding cavity. Although squalene lacks polar functional groups capable of forming hydrogen bonds with the serine and glutamate residues critical to native ligand recognition, its elongated polyisoprene chain ($C_{30}H_{50}$) appears to achieve favorable van der Waals complementarity with the hydrophobic lining of the ATP-binding region. This finding aligns with its documented enrichment in *S. tonkinensis* extracts as identified in the GC-MS analysis.

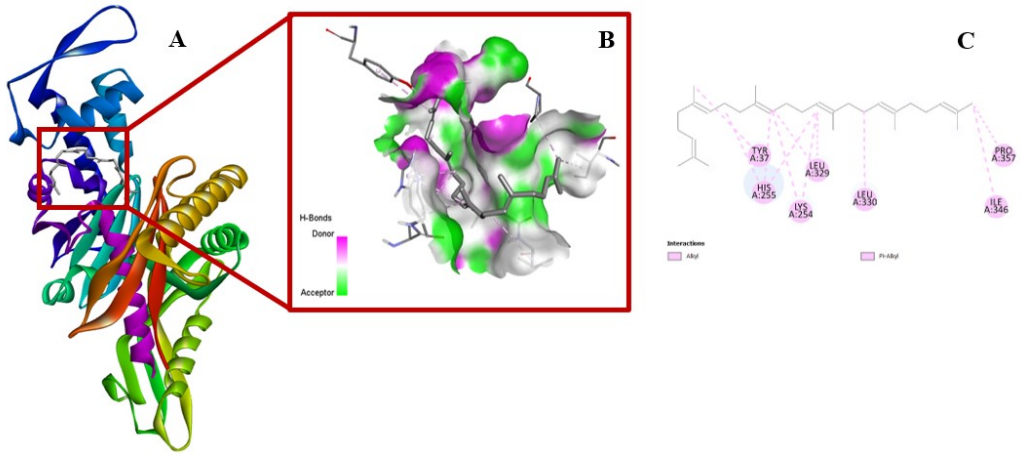

Figure 7. Docking model of squalene bound to 3WT0. (A) Overall protein structure showing the ligand-binding region. (B) 3D view of the docked complex within the binding pocket. (C) 2D interaction map illustrating hydrophobic interactions between squalene and key amino acid residues of 3WT0.

Phytol (-6.7 kcal/mol) engaged the widest repertoire of FtsA residues among all test compounds, establishing conventional hydrogen bonds with VAL211 and ASP206, alkyl and pi-alkyl interactions with HIS255, LEU329, and LYS254, and van der Waals contacts spanning twelve additional residues including SER13, SER14, GLU209, GLY325, ASN328, and the Mg cofactor. Despite this broad engagement, the presence of an unfavorable donor-donor interaction at GLY208 may partially attenuate phytol's binding effectiveness, as such repulsive contacts introduce destabilizing electrostatic forces within the binding interface and may limit precise complementarity with the active site geometry (Grassmann et al., 2023). This finding provides a mechanistic rationale for phytol's moderate affinity at this target notwithstanding its numerous contact residues.

Of particular mechanistic interest, 2-THP (-5.7 kcal/mol) reproduced the hydrogen bonding pattern most closely resembling the native ligand, forming conventional hydrogen bonds with SER13, GLU209, ASP210, and VAL211, the same acidic and hydroxyl residues engaged by the co-crystallized compound. The simultaneous alkyl interaction with PRO79 indicates orientation of the propionyl side chain toward a hydrophobic peripheral region of the binding cavity. Although 2-THP achieves the weakest binding among those that replicate polar interactions at FtsA, its structural mimicry of native ligand contacts at catalytic residues may be mechanistically significant. The small molecular size of 2-THP (MW 139.19 g/mol) likely limits the total interaction energy achievable, yet the selectivity of its hydrogen bond pattern toward ASP210 and GLU209, residues critical for catalytic coordination, warrants attention as a basis for structural optimization. This observation parallels the mechanism reported for THP derivatives as efflux pump modulators, where the nitrogen-containing ring engages polar protein residues even at low molecular weight (Ramis et al., 2019).

Stigmasterol (-5.6 kcal/mol) and lupeol (-5.3 kcal/mol) showed comparatively weaker FtsA interactions, with stigmasterol forming a conventional hydrogen bond with GLU209 alongside pi-sigma interactions at HIS255 and hydrophobic contacts at TYR37 and LYS252, while lupeol engaged TYR37, HIS255, and LYS252 through pi-sigma and alkyl contacts. The planar steroidal and pentacyclic triterpenoid frameworks of stigmasterol and lupeol, respectively, appear less geometrically compatible with the elongated ATP-binding cleft of FtsA than the linear polyisoprene scaffold of squalene, accounting for their relatively lower affinity at this target.

Binding at OmpF (PDB: 4KR4)

OmpF is a trimeric outer membrane porin of Gram-negative bacteria that facilitates the passive diffusion of hydrophilic molecules, including many antibiotics, across the outer membrane (Gao et al., 2025). Modulation of OmpF through ligand occupancy may alter membrane permeability and influence antibiotic susceptibility (Donoghue et al., 2023). The native ligand binds primarily through electrostatic interactions involving ARG77, LYS16, ARG60, and ARG20, reflecting the ionic character of the OmpF channel.

The detailed interaction profiles of the selected compounds with OmpF are summarized in Table 7. Unlike the native ligand, all tested compounds interacted with TYR112 through alkyl and π-alkyl contacts, indicating a shared binding mode within a predominantly hydrophobic region of the OmpF constriction zone. This suggests that these natural compounds may influence channel permeability through steric and hydrophobic effects rather than electrostatic interactions.

Among the evaluated ligands, lupeol exhibited the strongest binding affinity (-8.0 kcal/mol), surpassing that of the native ligand (-7.3 kcal/mol), followed by stigmasterol (-7.7 kcal/mol). As illustrated in Figure 8, lupeol occupied the constriction region of the OmpF channel and established predominantly hydrophobic interactions within the binding pocket. The superior affinity of lupeol and stigmasterol likely reflects

favorable size complementarity between their rigid polycyclic structures and the topology of the OmpF constriction region, resulting in strong hydrophobic stabilization. The strong binding of lupeol despite its relatively simple interaction profile may further indicate substantial van der Waals complementarity within the channel interior (Gao et al., 2025).

Table 7. Detailed ligand–protein interaction analysis of the selected compounds and native ligand within the binding pocket of 4KR4.

Receptor	Amino acid	Native Ligand	Lupeol	2-THP	Squalene	Phytol	Stigmasterol
4KR4	ARG77						
	LYS16						
	ARG60						
	ARG20						
	TYR112						
	SER114						
	PHE113						
	GLU116						
	TYR97						
	TYR101						
	VAL22						

Interaction

- Conventional Hydrogen Bond
- Van der Waals
- Carbon Hydrogen Bond
- Salt Bridge / Attractive Charge / Pi-Anion/Cation
- Pi-Sigma
- Alkyl / Pi-Alkyl
- Unfavorable Interaction

OmpF modulation by terpenoids is pharmacologically relevant, as porin-mediated permeability directly influences antibiotic susceptibility in Gram-negative bacteria (Boi et al., 2025). The strong affinity of stigmasterol at OmpF is consistent with its documented antibacterial activity (Demgne et al., 2022). In contrast, 2-THP showed the weakest binding affinity (-4.4 kcal/mol) but formed conventional hydrogen bonds with SER114, PHE113, and GLU116 in addition to an alkyl interaction with TYR112. Although these interactions suggest a distinct binding mechanism, the relatively weak binding energy indicates limited pharmacological relevance toward OmpF modulation.

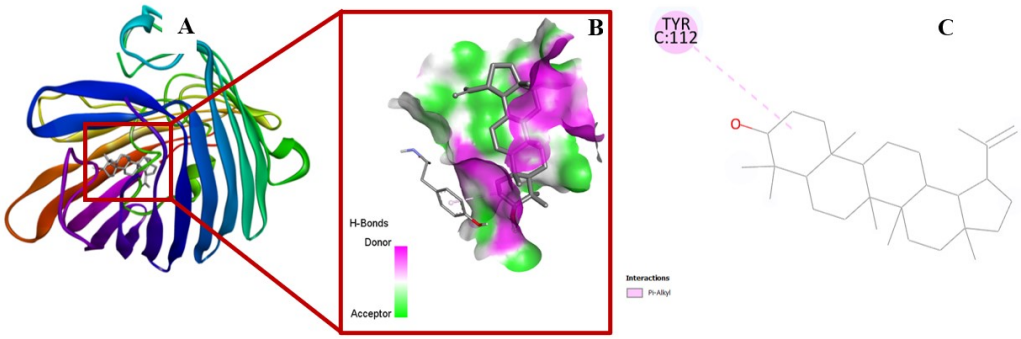

Figure 8. Molecular docking visualization of the lupeol–4KR4 complex. (A) Overall binding pose of lupeol within the 4KR4 binding region. (B) 3D representation of the ligand–protein interactions within the binding pocket. (C) 2D interaction map showing the amino acid residues and intermolecular interactions involved in stabilization of the lupeol–4KR4 complex.

Binding at GyrB (PDB: 6KZV)

DNA gyrase is a type II topoisomerase composed of two A (GyrA) and two B (GyrB) subunits, forming an A_2B_2 heterotetramer essential for bacterial DNA replication. The GyrB subunit contains the ATPase domain responsible for ATP hydrolysis during DNA supercoiling, making it an established target of antibacterial agents such as novobiocin (Gupta et al., 2021). The ATP-binding pocket of GyrB (PDB: 6KZV) comprises conserved hydrophobic residues including ILE78, VAL120, PRO79, ILE94, ALA47, and VAL167, together with catalytic residues ASP73 and GLU50 that are critical for ATP binding and hydrolysis.

The detailed interaction profiles of the selected compounds with GyrB are summarized in Table 8. The native ligand established a conventional hydrogen bond with ASP73, π-anion interaction with GLU50, π-cation interaction with ARG76, and hydrophobic contacts with ILE78, ALA47, VAL120, PRO79, and ILE94. This combination of polar and hydrophobic interactions characterizes the binding mode required for effective GyrB inhibition.

Table 8. Detailed ligand–protein interaction analysis of the selected compounds and native ligand within the ATP-binding pocket of 6KZV.

Receptor	Amino acid	Native Ligand	Lupeol	2-THP	Squalene	Phytol	Stigmasterol
6KZV	ASP73						
	GLU50						
	ARG76						
	ILE78						
	ALA47						
	VAL120						
	PRO79						
	ILE94						
	VAL167						
	VAL43						
	VAL71						
	ALA53						

Interaction

- Conventional Hydrogen Bond
- Van der Waals
- Carbon Hydrogen Bond
- Salt Bridge / Attractive Charge / Pi-Anion/Cation
- Pi-Sigma
- Alkyl / Pi-Alkyl
- Unfavorable Interaction

Among the tested compounds, stigmasterol (-7.9 kcal/mol) and lupeol (-7.6 kcal/mol) exhibited the strongest binding affinities, both interacting with the conserved hydrophobic triad of ILE78, VAL120, and PRO79 through alkyl and π-alkyl contacts. Stigmasterol additionally interacted with VAL167, whereas lupeol extended its contacts to ILE94, partially reproducing the interaction pattern of the native ligand. As illustrated in Figure 9, stigmasterol occupied the ATP-binding pocket and established extensive hydrophobic interactions that contributed to favorable complex stabilization. The binding of these pentacyclic terpenoids is consistent with previous reports demonstrating the ability of terpenoid natural products to inhibit enzymes involved in DNA metabolism, such as DNA polymerases and reverse transcriptases, by interacting with nucleotide-binding sites, this suggests a potential for terpenoids to target ATP-binding regions in other enzymes (Wu et al., 2020).

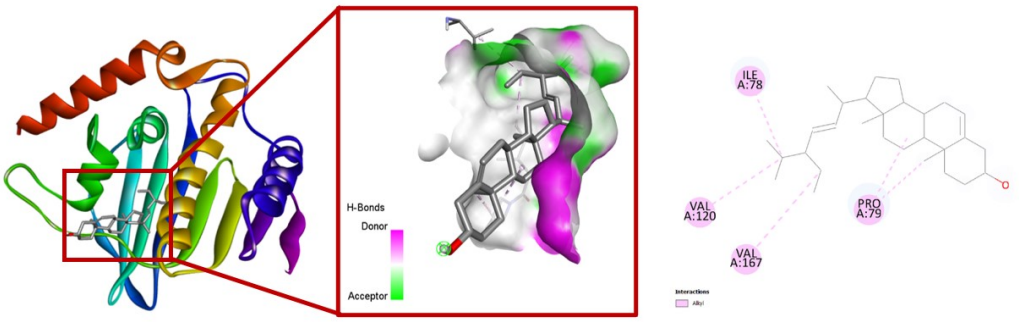

Figure 9. Molecular docking visualization of the stigmasterol–6KZV complex. (A) Overall binding pose of stigmasterol within the ATP-binding pocket of 6KZV. (B) Three-dimensional representation of the ligand–protein interactions within the binding site. (C) Two-dimensional interaction map showing the amino acid residues and intermolecular interactions involved in stabilization of the stigmasterol–6KZV complex.

Notably, 2-THP was the only test compound to reproduce the conventional hydrogen bond with ASP73 observed for the native ligand, in addition to a carbon hydrogen bond with VAL43. Although its overall binding affinity was the weakest among the tested compounds (-5.4 kcal/mol), interaction with the catalytic ASP73 residue suggests a distinct yet potentially relevant binding mode. The convergence of ASP73 hydrogen

bonding between the native ligand and 2-THP indicates possible competition for the catalytic region, although the limited hydrophobic contacts reduce its overall binding strength. This observation is consistent with reports describing the biological activity of THP derivatives against bacterial targets (Al-Juboori, 2020).

Phytol (-6.4 kcal/mol) and squalene (-6.3 kcal/mol) occupied the GyrB hydrophobic pocket through alkyl and π-alkyl interactions with residues including ILE78, VAL120, PRO79, ILE94, VAL167, and VAL43. Phytol additionally interacted with ALA47 and partially reproduced the binding geometry of the native ligand, consistent with recent studies reporting its inhibitory potential against GyrB-related targets (Saini et al., 2024). In contrast, the linear structure of squalene appears less compatible with the compact ATP-binding pocket of GyrB than the rigid polycyclic frameworks of stigmasterol and lupeol, providing a structural explanation for its comparatively lower binding affinity.

Multi-target Antibacterial Potential and Mechanistic Implications

The binding profiles across three distinct bacterial targets suggest that the selected compounds from *S. tonkinensis* may exert antibacterial effects through multi-target mechanisms rather than single-target inhibition. Among the evaluated compounds, lupeol and stigmasterol demonstrated the most promising profiles, exhibiting strong binding toward both OmpF and GyrB, which may contribute to simultaneous modulation of outer membrane permeability and inhibition of DNA replication. Such multi-target activity is considered advantageous for reducing the likelihood of resistance development (Banjare et al., 2023). Notably, stigmasterol was the dominant constituent of the n-hexane Soxhlet extract (67.95%) and was consistently detected across all extraction methods, linking its favorable docking performance directly to the phytochemical composition of *S. tonkinensis*. Likewise, squalene, a characteristic metabolite of the species, exhibited the strongest binding toward FtsA among the tested compounds, suggesting a potential role in disrupting bacterial cell division. Collectively, these findings provide mechanistic support for the traditional use of *S. tonkinensis* in Karo herbal medicine and identify its major lipophilic metabolites as promising candidates for further antibacterial investigation.

Drug-Likeness, Pharmacokinetic, and Toxicity Prediction

The selected compounds used for molecular docking were identified based on their abundance, structural diversity, and reported biological activities. Their PubChem identifiers, molecular formulas, and molecular weights are summarized in Table 9.

Table 9. Selected compounds identified for molecular docking and ADMET analysis, including PubChem CID, molecular formula, and molecular weight.

Compound	PubChem CID	Formula	MW (g/mol)
Stigmasterol	5280794	$C_{29}H_{48}O$	412.69
Phytol	5280435	$C_{20}H_{40}O$	296.53
Lupeol	259846	$C_{30}H_{50}O$	426.72
Squalene	638072	$C_{30}H_{50}$	410.72
2-Propionyl-1,4,5,6-tetrahydropyridine	522742	$C_8H_{13}NO$	139.19

The predicted drug-likeness and pharmacokinetic properties of the selected compounds are presented in Table 10.

Table 10. Predicted drug-likeness and pharmacokinetic properties of selected compounds based on SwissADME analysis.

Compound	MW	TPSA (Å^2)	HBA	HBD	XLogP3	GI Absorption	BBB Permeability	Lipinski Violations
Stigmasterol	412.69	20.23	1	1	8.56	Low	No	1
Phytol	296.53	20.23	1	1	8.19	Low	No	1
Lupeol	426.72	20.23	1	1	9.87	Low	No	1
Squalene	410.72	0.00	0	0	11.58	Low	No	1
2-Propionyl-1,4,5,6-tetrahydropyridine	139.19	29.10	2	0	1.53	High	Yes	0

Among the evaluated compounds, 2-propionyl-1,4,5,6-tetrahydropyridine (2-THP) was the only compound that fully complied with Lipinski's Rule of Five, exhibiting low molecular weight (139.19 g/mol), moderate lipophilicity (XLogP3 = 1.53), high gastrointestinal absorption, and predicted BBB permeability. In contrast, stigmasterol, phytol, lupeol, and squalene each showed one Lipinski violation due to excessive lipophilicity (XLogP3 > 5), resulting in low predicted GI absorption and lack of BBB penetration. Among these compounds, squalene exhibited the highest lipophilicity (XLogP3 = 11.58) and the lowest polarity

(TPSA = 0 Å²), reflecting its highly hydrophobic character. Although these properties may limit oral bioavailability, highly lipophilic terpenoids and phytosterols frequently retain pharmacological relevance through lipid-assisted absorption, alternative delivery systems, or local gastrointestinal activity (Li et al., 2022; Zhao et al., 2026). When considered together with the docking results, stigmasterol and lupeol displayed the most favorable antibacterial binding profiles, whereas 2-THP demonstrated the most advantageous pharmacokinetic characteristics. The predicted toxicity profiles of the selected compounds obtained from ProTox 3.0 are summarized in Table 11.

Table 11. Predicted acute toxicity, hepatotoxicity, and carcinogenicity profiles of selected compounds obtained from ProTox-3.0.

Compound	LD50 (mg/kg)	Toxicity Class	Hepatotoxicity	Carcinogenicity
Stigmasterol	890	4	Inactive (0.87)	Inactive (0.60)
Phytol	5000	5	Inactive (0.79)	Inactive (0.76)
Lupeol	2000	4	Inactive (0.91)	Inactive (0.63)
Squalene	5000	5	Inactive (0.79)	Inactive (0.76)
2-Propionyl-1,4,5,6-tetrahydropyridine	825	4	Inactive (0.66)	Inactive (0.67)

All compounds exhibited favorable preliminary safety profiles, with inactive predictions for both hepatotoxicity and carcinogenicity. Phytol and squalene showed the lowest predicted acute toxicity, with LD50 values of 5000 mg/kg and classification in toxicity class V. Meanwhile, stigmasterol, lupeol, and 2-THP were assigned to toxicity class IV, with LD50 values ranging from 825 to 2000 mg/kg. Although these predictions require experimental validation, the absence of predicted hepatotoxic and carcinogenic effects, together with acceptable acute toxicity profiles, suggests that the major metabolites of *S. tonkinensis* possess promising safety characteristics for further antibacterial investigation.

Collectively, the molecular docking, ADME, and toxicity analyses identified lupeol and stigmasterol as the most promising antibacterial candidates from *S. tonkinensis*, owing to their strong binding affinities toward multiple bacterial targets and favorable preliminary safety profiles despite limited oral bioavailability associated with high lipophilicity. Nevertheless, these findings should be interpreted as preliminary computational evidence, and further validation through in vitro antibacterial assays, pharmacokinetic studies, and toxicity evaluations is required to confirm their therapeutic potential.

CONCLUSIONS

GC–MS profiling demonstrated that the metabolite composition of *Strobilanthes tonkinensis* leaves was strongly influenced by extraction method, solvent polarity, and leaf condition. Fresh leaf extracts were enriched in nitrogen-containing compounds, with 2-propionyl-1,4,5,6-tetrahydropyridine identified as the major constituent, whereas dried leaf extracts were dominated by lipophilic terpenoids and phytosterols. n-Hexane Soxhlet extraction provided the highest enrichment of stigmasterol (67.95%), while squalene was detected exclusively in maceration extracts. Molecular docking revealed that lupeol and stigmasterol exhibited the most favorable multi-target antibacterial potential against OmpF and DNA gyrase B, whereas squalene showed the strongest affinity toward FtsA. ADME prediction identified 2-THP as the compound with the most favorable pharmacokinetic profile, while toxicity prediction indicated that all selected compounds were non-hepatotoxic and non-carcinogenic. These findings provide integrated GC–MS and in silico antibacterial characterization of *S. tonkinensis* and support lupeol and stigmasterol as priority candidates for further in vitro and in vivo validation. Future studies should focus on experimental MIC determination, membrane permeability assays, and bioavailability enhancement strategies for the identified terpenoid leads.

Acknowledgements: The authors acknowledge financial support from the Penelitian Dosen Pemula (PDP) Grant Scheme, Institute for Research and Community Service (LPPM), Universitas Negeri Medan, under Contract No. **025/UN33.8/PPKM/PDP/2026**. The authors are also grateful to the Organic Chemistry Laboratory and Biology Laboratory, FMIPA Universitas Negeri Medan, for providing research facilities and GC–MS instrumentation, respectively, and to Herbarium Medanense (MEDA), Universitas Sumatera Utara, for plant identification and authentication services.

Authors' Contributions: D.S.R. conceived the research idea, designed the study, supervised all research activities, secured funding, analyzed and interpreted the data, and drafted the manuscript. D.W. and H.H. contributed to research design, data interpretation, and critical revision of the manuscript. T.J. contributed to methodology development and scientific review of the manuscript. R.N.E.S. carried out sample preparation, extraction, and laboratory experiments. V.O.A.

conducted molecular docking and ADMET analyses and assisted in data interpretation. I.S. provided technical support for GC–MS analysis and instrumentation. All authors read, reviewed, and approved the final manuscript.

Competing Interests: The authors declare that there are no competing interests related to the content of this manuscript.

Funding: This research was funded by the Penelitian Dosen Pemula (PDP) Grant Scheme, Institute for Research and Community Service (LPPM), Universitas Negeri Medan, Indonesia, under Contract No. 025/UN33.8/PPKM/PDP/2026.

REFERENCES

Abdullah Sani, M. S., Bakar, J., Abdul Rahman, R., & Abas, F. (2021). Antibacterial composition of bioautographic fractions, characteristics, and stability of Carica papaya seed extract. *International Food Research Journal*, *28*(3), 443–456. https://doi.org/10.47836/ifrj.28.3.04

Abedelmaksoud, T. G., Younis, M. I., Altemimi, A. B., Tlay, R. H., & Ali Hassan, N. (2025). Bioactive Compounds of Plant-Based Food: Extraction, Isolation, Identification, Characteristics, and Emerging Applications. *Food Science & Nutrition*, *13*(6). https://doi.org/10.1002/fsn3.70351

Al-Juboori, S. B. (2020). Synthesis, Antimicrobial Evolution, Defibrillation Threshold Studies, Docking Studies, Silico Admet Analysis and PER-Metabolism Study of Some New Dihydropyrmidine Derivatives. *International Journal of Drug Delivery Technology*, *10*(01), 21–32. https://doi.org/10.25258/ijddt.10.1.5

Almeida-Bezerra, J. W., Menezes, S. A., Silva, J. T. da C., de Sousa, S. G., Alves, D. S., Alencar, G. G., Araújo, I. M., Rodrigues, E. Y. de S., Oliveira-Tintino, C. D. de M., da Cruz, R. P., Rocha, J. E., Tintino, S. R., Barbosa-Filho, J. M., Morais-Braga, M. F. B., de Menezes, I. R. A., Raposo, A., & Coutinho, H. D. M. (2024). Analysis of the Antibiotic-Potentiating Activity, Absorption, Distribution, Metabolism, and Excretion (ADME) and the Molecular Docking Properties of Phytol Against Multi-Drug-Resistant (MDR) Strains. *Antibiotics*, *13*(12), 1171. https://doi.org/10.3390/antibiotics13121171

Al-Rooqi, M. M., Ullah Mughal, E., Raja, Q. A., Obaid, R. J., Sadiq, A., Naeem, N., Qurban, J., Asghar, B. H., Moussa, Z., & Ahmed, S. A. (2022). Recent advancements on the synthesis and biological significance of pipecolic acid and its derivatives. *Journal of Molecular Structure*, *1268*, 133719. https://doi.org/10.1016/j.molstruc.2022.133719

Azzahra, V. O., Mardiana, S., Sianipar, R. J., & Ramadhan, D. S. (2025). Effect of Solvent Polarity on Extraction Yield, Phytochemical Composition, and Antioxidant Activity of Curcuma xanthorrhiza Roxb. and Moringa oleifera Lam. *Biology, Medicine, & Natural Product Chemistry*, *14*(2), 1273–1284. https://doi.org/10.14421/biomedich.2025.142.1273-1284

Bakrim, S., Benkhaira, N., Bourais, I., Benali, T., Lee, L.-H., El Omari, N., Sheikh, R. A., Goh, K. W., Ming, L. C., & Bouyahya, A. (2022). Health Benefits and Pharmacological Properties of Stigmasterol. *Antioxidants*, *11*(10), 1912. https://doi.org/10.3390/antiox11101912

Banerjee, P., Kemmler, E., Dunkel, M., & Preissner, R. (2024). ProTox 3.0: a webserver for the prediction of toxicity of chemicals. *Nucleic Acids Research*, *52*(W1), W513–W520. https://doi.org/10.1093/nar/gkae303

Banjare, P., Wamanrao Matore, B., Murmu, A., Kumar, V., Singh, J., & Roy, P. P. (2023). In silico Strategy: A Promising Implement in the Development of Multitarget Drugs against Neurodegenerative Diseases. *Current Topics in Medicinal Chemistry*, *23*(29), 2765–2791. https://doi.org/10.2174/1568026623666230811113231

Boi, S., Puxeddu, S., Delogu, I., Farci, D., Piano, D., Manzin, A., Ceccarelli, M., Angius, F., Scorciapino, M. A., & Milenkovic, S. (2025). Seeking Correlation Among Porin Permeabilities and Minimum Inhibitory Concentrations Through Machine Learning: A Promising Route to the Essential Molecular Descriptors. *Molecules*, *30*(6), 1224. https://doi.org/10.3390/molecules30061224

Boufissiou, A., Abdalla, M., Kadi, I., Soumaya, H., Eltayb, W. A., Awadalla, M. E., Algarni, A. S., Benarfa, A., Bouchareb, A., Benaceur, F., & Berrabah, F. (2025). Identification of natural product inhibitors as potential drug candidates for treating Alzheimer's disease: molecular docking, molecular dynamics simulations, MM/GBSA and pharmacokinetics. *Network Modeling Analysis in Health Informatics and Bioinformatics*, *14*(1), 56. https://doi.org/10.1007/s13721-025-00543-z

Cameron, T. A., & Margolin, W. (2023). Construction and Characterization of Functional FtsA Sandwich Fusions for Studies of FtsA Localization and Dynamics during Escherichia coli Cell Division. *Journal of Bacteriology*, *205*(1). https://doi.org/10.1128/jb.00373-22

Chaudhary, G., Verma, A., Maurya, S., Singh, R., Tyagi, S., Manna, B., Katara, P., Prabhakar, A., Verma, D., & Bihari Yadav, A. (2026). Design, Synthesis, and Biological Evaluation of Tetrahydropyridine Analogues as Potent Antibiofilm Agents against *S. aureus* : In Vitro and In Silico Studies. *ACS Omega*, *11*(1), 476–489. https://doi.org/10.1021/acsomega.5c05577

Demgne, O. M. F., Mbougnia, J. F. T., Seukep, A. J., Mbaveng, A. T., Tene, M., Nayim, P., Wamba, B. E. N., Guefack, M.-G. F., Beng, V. P., Tane, P., & Kuete, V. (2022). Antibacterial phytocomplexes and compounds from Psychotria sycophylla (Rubiaceae) against drug-resistant bacteria. *Advances in Traditional Medicine*, *22*(4), 761–772. https://doi.org/10.1007/s13596-021-00608-0

Desbois, A. P., & Smith, V. J. (2010). Antibacterial free fatty acids: activities, mechanisms of action and biotechnological potential. *Applied Microbiology and Biotechnology*, *85*(6), 1629–1642. https://doi.org/10.1007/s00253-009-2355-3

Donoghue, A., Winterhalter, M., & Gutsmann, T. (2023). Influence of Membrane Asymmetry on OmpF Insertion, Orientation and Function. *Membranes*, *13*(5), 517. https://doi.org/10.3390/membranes13050517

Fatmayanti, B. R., Jumina, Purwono, B., Kurniawan, Y. S., Pranowo, H. D., & Sholikhah, E. N. (2024). Oleate Epoxides Derived from Palm Oil as New Anticancer Agents: Synthesis, Cytotoxicity Evaluation, and Molecular Docking Studies Against FASN Protein. *ChemistrySelect*, *9*(17). https://doi.org/10.1002/slct.202400752

Ganesan, T., Subban, M., Christopher Leslee, D. B., Kuppannan, S. B., & Seedevi, P. (2024). Structural characterization of n-hexadecanoic acid from the leaves of Ipomoea eriocarpa and its antioxidant and antibacterial activities. *Biomass Conversion*

and Biorefinery, *14*(13), 14547–14558. https://doi.org/10.1007/s13399-022-03576-w

Gao, Y., Widmalm, G., & Im, W. (2025). Dynamics and Interactions of OmpF Porin in an Asymmetric Bacterial Outer Membrane including LPS, ECA, and CPS. *Biomacromolecules*, *26*(6), 3711–3720. https://doi.org/10.1021/acs.biomac.5c00285

Grassmann, G., Di Rienzo, L., Gosti, G., Leonetti, M., Ruocco, G., Miotto, M., & Milanetti, E. (2023). Electrostatic complementarity at the interface drives transient protein-protein interactions. *Scientific Reports*, *13*(1), 10207. https://doi.org/10.1038/s41598-023-37130-z

Gupta, D., Tiwari, P., Haque, M. A., Sachdeva, E., Hassan, M. I., Ethayathulla, A. S., & Kaur, P. (2021). Structural insights into the transient closed conformation and pH dependent ATPase activity of S.Typhi GyraseB N- terminal domain. *Archives of Biochemistry and Biophysics*, *701*, 108786. https://doi.org/10.1016/j.abb.2021.108786

Hartavi, A. (2025). Onosma obtusifolia extracts: Antioxidant potential and molecular docking insights into acetylcholinesterase, α-amylase, and tyrosinase inhibition. *Industrial Crops and Products*, *233*, 121387. https://doi.org/10.1016/j.indcrop.2025.121387

Hartmann, M., Kim, D., Bernsdorff, F., Ajami-Rashidi, Z., Scholten, N., Schreiber, S., Zeier, T., Schuck, S., Reichel-Deland, V., & Zeier, J. (2017). Biochemical Principles and Functional Aspects of Pipecolic Acid Biosynthesis in Plant Immunity. *Plant Physiology*, *174*(1), 124–153. https://doi.org/10.1104/pp.17.00222

Hua, J., Li, J., Ouyang, W., Wang, J., Yuan, H., & Jiang, Y. (2022). Effect of Strobilanthes tonkinensis Lindau Addition on Black Tea Flavor Quality and Volatile Metabolite Content. *Foods*, *11*(12), 1678. https://doi.org/10.3390/foods11121678

Karuppiah, V., & Seralathan, M. (2022). Quorum sensing inhibitory potential of vaccenic acid against Chromobacterium violaceum and methicillin-resistant Staphylococcus aureus. *World Journal of Microbiology and Biotechnology*, *38*(8), 146. https://doi.org/10.1007/s11274-022-03335-z

Kato, K., Ishido, T., Matsui, T., & Yao, M. (2015). Crystal Structure Analysis of Cell Division Protein. In *Worldwide Protein Data Bank*. https://doi.org/10.2210/pdb3wt0/pdb

Khan, T., Tanveer, S., Hashmi, K., Veg, E., Ahmad, M. I., & Mishra, N. (2025). Lupeol as Antimicrobial Agent. In *Lupeol* (pp. 145–160). CRC Press. https://doi.org/10.1201/9781003600022-12

Khan, U., HAYAT, F., KHANUM, F., AHMED, N., ABDİN, M., ABDALMEGEED, D., KARATAŞ, N., & XİN, Z. (2023). Exploring the diverse applications of Stigmasterol from plants: A comprehensive review. *Turkish Journal of Agriculture and Forestry*, *47*(6), 801–816. https://doi.org/10.55730/1300-011X.3129

Kim, J., Choi, Y., Yu, H., & Chang, P. (2024). Lipase-catalyzed synthesis of erythorbyl oleate and its characterization as a multifunctional emulsifier. *Journal of Food Science*, *89*(11), 7324–7335. https://doi.org/10.1111/1750-3841.17413

Kim, Y. A., & Kim, H. K. (2025). Antibacterial Activity of a Linolenic Acid Stigmasterol Ester Produced by Lipase-Mediated Transesterification. *Journal of Microbiology and Biotechnology*, *35*, e2410055. https://doi.org/10.4014/jmb.2410.10055

Kurnia, D., Hutabarat, G. S., Windaryanti, D., Herlina, T., Herdiyati, Y., & Satari, M. H. (2020). Potential Allylpyrocatechol Derivatives as Antibacterial Agent Against Oral Pathogen of S. sanguinis ATCC 10,556 and as Inhibitor of MurA Enzymes: in vitro and in silico Study . *Drug Design, Development and Therapy*, *Volume 14*, 2977–2985. https://doi.org/10.2147/DDDT.S255269

Lee, W., Woo, E.-R., & Lee, D. G. (2016). Phytol has antibacterial property by inducing oxidative stress response in *Pseudomonas aeruginosa*. *Free Radical Research*, *50*(12), 1309–1318. https://doi.org/10.1080/10715762.2016.1241395

Lestari, S., Kurnia, D., Mayanti, T., & Heliawati, L. (2024). Antimicrobial Activities of Stigmasterol from *Piper crocatum In Vitro* and *In Silico*. *Journal of Chemistry*, *2024*(1). https://doi.org/10.1155/2024/2935516

Li, X., Xin, Y., Mo, Y., Marozik, P., He, T., & Guo, H. (2022). The Bioavailability and Biological Activities of Phytosterols as Modulators of Cholesterol Metabolism. *Molecules*, *27*(2), 523. https://doi.org/10.3390/molecules27020523

Liu, W., Liu, Z., Liu, H., Westerhoff, L. M., & Zheng, Z. (2022). Free Energy Calculations Using the Movable Type Method with Molecular Dynamics Driven Protein–Ligand Sampling. *Journal of Chemical Information and Modeling*, *62*(22), 5645–5665. https://doi.org/10.1021/acs.jcim.2c00278

Madhuranayaki, T., Balasubramaniam, D., & Krishnaswamy, S. (2014). Salmonella typhi OmpF complex with Ampicillin. In *Worldwide Protein Data Bank*. https://doi.org/10.2210/pdb4kr4/pdb

Mima, M., & Ushiyama, F. (2020). Crystal structure of E.coli DNA gyrase B in complex with 2-oxo-1,2-dihydroquinoline derivative. In *Worldwide Protein Data Bank*. https://doi.org/10.2210/pdb6kzv/pdb

Mohammad, M. K., Hussain, S. S., & Mahdi, A. S. (2025). Antibacterial and Anticancer Activities of Bioactive Compounds Produced by Bacillus thermoamylovorans. *International Journal of Design & Nature and Ecodynamics*, *20*(11), 2711–2718. https://doi.org/10.18280/ijdne.201122

Morgan, L. V., Petry, F., Scatolin, M., de Oliveira, P. V., Alves, B. O., Zilli, G. A. L., Volfe, C. R. B., Oltramari, A. R., de Oliveira, D., Scapinello, J., & Müller, L. G. (2021). Investigation of the anti-inflammatory effects of stigmasterol in mice: insight into its mechanism of action. *Behavioural Pharmacology*, *32*(8), 640–651. https://doi.org/10.1097/FBP.0000000000000658

Murray, C. J. L., Ikuta, K. S., Sharara, F., Swetschinski, L., Robles Aguilar, G., Gray, A., Han, C., Bisignano, C., Rao, P., Wool, E., Johnson, S. C., Browne, A. J., Chipeta, M. G., Fell, F., Hackett, S., Haines-Woodhouse, G., Kashef Hamadani, B. H., Kumaran, E. A. P., McManigal, B., … Naghavi, M. (2022). Global burden of bacterial antimicrobial resistance in 2019: a systematic analysis. *The Lancet*, *399*(10325), 629–655. https://doi.org/10.1016/S0140-6736(21)02724-0

Murugan, S., Karuppiah, V., Pandi, S., Govindasamy, M., & Thangavel, K. (2025). Bioactive Phytol from Thymus vulgaris, a promising source of alternative medicine to combat blaKPC and blaOXA-48 genotypes of Klebsiella pneumoniae: A retrospective in vitro and in silico approach. *Microbial Pathogenesis*, *206*, 107813. https://doi.org/10.1016/j.micpath.2025.107813

Newman, D. J., & Cragg, G. M. (2020). Natural Products as Sources of New Drugs over the Nearly Four Decades from 01/1981 to 09/2019. *Journal of Natural Products*, *83*(3), 770–803. https://doi.org/10.1021/acs.jnatprod.9b01285

Odoma, S., Adekilekun, A. H., Onohuean, H., Funso, F.-B., Oyewusi, A. H., & Hamid, A. A. (2025). GC-MS Determination of Bioactive Components with Their Biological Activities of Olax subscorpioidea (Olacaceae). *Biology,*

Medicine, & Natural Product Chemistry, *14*(2), 1437–1449. https://doi.org/10.14421/biomedich.2025.142.1437-1449

Park, Y. J., Park, D. H., & Bae, J.-S. (2024). Anti-Inflammatory Effects of Lupeol as a Candidate for New Drug Development. *The American Journal of Chinese Medicine*, *52*(06), 1759–1771. https://doi.org/10.1142/S0192415X2450068X

Puri, B., Vaishya, R., & Vaish, A. (2025). Antimicrobial resistance: Current challenges and future directions. *Medical Journal Armed Forces India*, *81*(3), 247–258. https://doi.org/10.1016/j.mjafi.2024.07.006

Raghavanpillai Sabu, K., Sugathan, S., Idhayadhulla, A., Woldemariam, M., Aklilu, A., Biresaw, G., Tsegaye, B., & Manilal, A. (2022). Antibacterial, Antifungal, and Cytotoxic Activity of Excoecaria agallocha Leaf Extract. *Journal of Experimental Pharmacology*, *Volume 14*, 17–26. https://doi.org/10.2147/JEP.S339383

Ramadhan, D. S., Warsito, W., Azzahra, V. O., Wardana, D., Fahmi, J., & Safitri, W. D. (2025). Comparative GC–MS Characterization and Physicochemical Evaluation Of *Citrus Hystrix* DC. Essential Oils From Different Plant Parts. *Walisongo Journal of Chemistry*, *8*(2), 192–203. https://doi.org/10.21580/wjc.v8i2.28063

Ramis, I. B., Vianna, J. S., Silva Junior, L., von Groll, A., Ramos, D. F., Lobo, M. M., Zanatta, N., Viveiros, M., & Silva, P. E. A. da. (2019). In silico and in vitro evaluation of tetrahydropyridine compounds as efflux inhibitors in Mycobacterium abscessus. *Tuberculosis*, *118*, 101853. https://doi.org/10.1016/j.tube.2019.07.004

Rawat, V., Kumar, R., Bhatt, P., Garzoli, S., Bargali, P., Negi, S., Kumar, A., Kumar, P., Chamoli, S., Gautam, S., & Rawat, D. S. (2026). Botanical, traditional uses, phytochemical and biological potential of Strobilanthes (Acanthaceae) – A review. *South African Journal of Botany*, *194*, 302–332. https://doi.org/10.1016/j.sajb.2026.05.008

Rossetti, A., Bono, N., Candiani, G., Meneghetti, F., Roda, G., & Sacchetti, A. (2019). Synthesis and Antimicrobial Evaluation of Novel Chiral 2-Amino-4,5,6,7-tetrahydrothieno[2,3- *c*]pyridine Derivatives. *Chemistry & Biodiversity*, *16*(6). https://doi.org/10.1002/cbdv.201900097

Saini, S., Tuli, H. S., Chauhan, R., Sharma, U., & Bansal, P. (2024). Ethyl Oleate, Hexadecenoic Acid, Phytol Profiling of Onosma bracteatum: Antibacterial, Anticancer and Molecular Docking Studies. *Asian Journal of Chemistry*, *36*(10), 2300–2306. https://doi.org/10.14233/ajchem.2024.32310

Salam, Md. A., Al-Amin, Md. Y., Salam, M. T., Pawar, J. S., Akhter, N., Rabaan, A. A., & Alqumber, M. A. A. (2023). Antimicrobial Resistance: A Growing Serious Threat for Global Public Health. *Healthcare*, *11*(13), 1946. https://doi.org/10.3390/healthcare11131946

Sarkar, A., Debnath, S., Das Chowdhury, B., Ghosh, R., & Debnath, B. (2024). Identification of phytoconstituents from Dicliptera paniculata and study of antibacterial activity guided by molecular docking. *In Silico Pharmacology*, *12*(1), 18. https://doi.org/10.1007/s40203-024-00196-2

Shamim, S., Munawar, R., Rashid, Y., Muhammad Zesshan Qadar, S., Bushra, R., Begum, I., Imran, M., & Quds, T. (2024). *Molecular Docking: An Insight from Drug Discovery to Drug Repurposing Approach*. https://doi.org/10.5772/intechopen.1005526

Sri Charan Bindu, B., Mishra, D. P., & Narayan, B. (2015). Inhibition of virulence of Staphylococcus aureus – a food borne pathogen – by squalene, a functional lipid. *Journal of Functional Foods*, *18*, 224–234. https://doi.org/10.1016/j.jff.2015.07.008

Srikun, N. (2017). In vitro propagation of the aromatic herb Strobilanthes tonkinensis Lindau. *Agriculture and Natural Resources*, *51*(1), 15–19. https://doi.org/10.1016/j.anres.2016.01.006

Steve, D., Kiarii, E. M., Kiarie, M. W., & Nyariki, J. N. (2026). Emergence and spread of multidrug-resistant pathogens: A global health challenge. *Mass Gathering Medicine*, *5*, 100050. https://doi.org/10.1016/j.mgmed.2026.100050

Suratman, S., Suranto, S., Muzzaninah, M., & Purnomo, P. (2022). Leaf anatomical characters variation of Strobilanthes s.l. from Sumatra, Indonesia and its taxonomic implications. *Biodiversitas Journal of Biological Diversity*, *23*(7). https://doi.org/10.13057/biodiv/d230748

Susawaengsup, C., Jaradrattanapaiboon, A., Sornsakdanuphap, J., Choengpanya, K., Jaradrattanapaiboon, Y., Tongkoom, K., & Bhuyar, P. (2022). Effect of Fertilization Combined with Shading on Growth and Aromatic Constituents of Niamhom (Strobilanthes nivea Craib) Using an Internet of Things (IoT) Controlled Irrigation System. *Horticulturae*, *8*(12), 1130. https://doi.org/10.3390/horticulturae8121130

Trott, O., & Olson, A. J. (2010). AutoDock Vina: Improving the speed and accuracy of docking with a new scoring function, efficient optimization, and multithreading. *Journal of Computational Chemistry*, *31*(2), 455–461. https://doi.org/10.1002/jcc.21334

Vianna, J. S., Ramis, I. B., Bierhals, D., von Groll, A., Ramos, D. F., Zanatta, N., Lourenço, M. C., Viveiros, M., & Almeida da Silva, P. E. (2019). Tetrahydropyridine derivative as efflux inhibitor in Mycobacterium abscessus. *Journal of Global Antimicrobial Resistance*, *17*, 296–299. https://doi.org/10.1016/j.jgar.2018.12.020

Wang, N., Zhang, J., Duan, Y., Zhu, R., Yang, L., Jiang, J., Li, H., Xu, Y., & Tai, Z. (2025). Ultrasound-Assisted Combined With Natural Ternary Deep Eutectic Solvent Extraction Method for the Green Extraction of Squalene From *Strobilanthes tonkinensis*. *Journal of Separation Science*, *48*(12). https://doi.org/10.1002/jssc.70332

Warsito, W., Murlistyarini, S., Suratmo, S., Azzahra, V., & Sucahyo, A. (2021). Molecular Docking Compounds of Cinnamaldehyde Derivatives as Anticancer Agents. *Asian Pacific Journal of Cancer Prevention*, *22*(8), 2409–2419. https://doi.org/10.31557/APJCP.2021.22.8.2409

Wu, Y., Hsieh, T., Wu, J. M., Wang, X., Christopher, J. S., Pham, A. H., Swaby, J. D.-L., Lou, L., & Xie, Z.-R. (2020). Elucidating the Inhibitory Effect of Resveratrol and Its Structural Analogs on Selected Nucleotide-Related Enzymes. *Biomolecules*, *10*(9), 1223. https://doi.org/10.3390/biom10091223

Yang, R., Zhang, L., Li, P., Yu, L., Mao, J., Wang, X., & Zhang, Q. (2018). A review of chemical composition and nutritional properties of minor vegetable oils in China. *Trends in Food Science & Technology*, *74*, 26–32. https://doi.org/10.1016/j.tifs.2018.01.013

Yang, X., He, X., Cui, Y., Ji, L., Hu, J., Hao, J., & He, B. (2025). Enhance rice-like aroma of on *Strobilanthes tonkinensis* var. *tonkinensis* extract using hydroxypropyl- β -cyclodextrin. *International Journal of Food Properties*, *28*(1). https://doi.org/10.1080/10942912.2025.2595770

Yasir, M., Patra, J., Maurya, R. K., Tripathi, A. S., & Pathan, H. K. (2025). Exploring natural products for allosteric inhibition of glutathione peroxidase 4 in drug-resistant cancers via molecular docking and dynamics. *Anti-Cancer Drugs*, *36*(9), 723–730. https://doi.org/10.1097/CAD.0000000000001749

Yuan, Y., Tarres, A., Bessaire, T., Stadler, R. H., & Delatour, T. (2017). Heat-induced formation of mepiquat by decarboxylation of pipecolic acid and its betaine derivative. Part 1: Model system studies. *Food Chemistry*, *227*, 173–178. https://doi.org/10.1016/j.foodchem.2017.01.095

Zhao, T., Wang, Z., Jiang, Y., Li, P., & Lu, B. (2026). Phytosterol intestinal absorption fate: The critical modulatory role of dietary fatty acids by multi-model evaluation. *Trends in Food Science & Technology*, *172*, 105645. https://doi.org/10.1016/j.tifs.2026.105645

Zhu, X., Xu, Y., Sun, D., Li, H., & Chen, L. (2022). The genus Strobilanthes: phytochemistry and pharmacology. *TMR Modern Herbal Medicine*, *5*(3), 15. https://doi.org/10.53388/MHM2022B0701001

Zulueta Díaz, Y. de las M., & Fanani, M. L. (2017). Crossregulation between the insertion of Hexadecylphosphocholine (miltefosine) into lipid membranes and their rheology and lateral structure. *Biochimica et Biophysica Acta (BBA) - Biomembranes*, *1859*(10), 1891–1899. https://doi.org/10.1016/j.bbamem.2017.06.008